A PRELIMINARY INVESTIGATION OF A UTIAS IMPLOSION-DRIVEN SHOCK TUBE

by

J. C. Poinssot

Manuscript received October, 1968.

July, 1969.

UTIAS Technical Note No. 136

A PRELIMINARY INVESTIGATION OF A UTIAS IMPLOSION-DRIVEN SHOCK TUBE

by

J. C. Poinssot

Manuscript received October, 1968.

July, 1969. UTIAS Technical Note No. 136

ACKNOWLEDGEMENTS

I wish to thank Dr. G. N. Patterson for the opportunity to conduct this work at the Institute for Aerospace Studies.

I should like to express my gratitude to Dr. I. I. Glass who suggested the problem. His supervision and advice throughout the course of this project are gratefully acknowledged.

Thanks are due to Dr. A. K. Roberts, A. Elsenaar and W. O. Graf, for many helpful discussions. The assistance of W. C. Burgess in carrying out the experimental work is very much appreciated.

I am very grateful to the "Conseil des Arts du Canada" for a scholarship which gave me this opportunity of studying in Canada.

The computer time provided by the Institute of Computer Science is acknowledged with thanks.

This work was financially supported by the Aerospace Research Laboratory of the United States Air Force under Contract No. AF 33(615)-5313.

SUMMARY

A detailed description is given of a program which has been developed to study analytically the performance of a UTIAS Implosion-Driven Shock Tube. Some results of the computations are presented. These have been checked experimentally using an existing 8 inch diameter implosion chamber and a 5/16 inch diameter channel. The experimentally measured shock-wave Mach numbers were much greater than anticipated from the computations. The cause of the discrepencies is shown to be largely computational, and recommendations to improve the calculations are proposed. The experimentally measured shock Mach numbers decrease quite rapidly in the 5/16 inch diameter tube, as expected. Nevertheless, it was possible to obtain a shock Mach number $M_s \simeq 40$ in air using only a 600 psi $2H_2 + O_2$ gaseous implosion driver. Much higher shock Mach numbers are expected with a coupled PETN explosive driver.

TABLE OF CONTENTS

1. INTRODUCTION

In order to overcome the current "performance barrier" of Hypervelocity Launchers, Professor I. I. Glass proposed in 1959 the use of spherical, imploding shock waves. Since then, the Institute for Aerospace Studies has been actively engaged in this field [1]. An Implosion-Driven Hypervelocity Launcher has been designed and Fig.1 illustrates schematically its principle of operation. A model with an 8 inch diameter hemispherical chamber has been built and several experimental studies are going on. A numerical model has also been developed and some previous investigations [2-3] have been concerned with the computed performance and the optimization of this launcher.

The present preliminary study deals mainly with the computation of the performance of an implosion-driven shock tube. The primary aim was to study analytically the limit of a launcher as the mass of the projectile goes to zero. Such a study should enable us to place an upper limit on the projectile velocities that could be attained with this type of hypervelocity launcher. It was thought also, following the first results, that an implosion-driven shock tube would be a good facility to obtain extremely high shock-wave Mach numbers at relatively high channel pressures.

An analytical investigation is presented here and is followed by some experimental results obtained in a 5/16 inch diameter channel (barrel) with an 8 inch diameter hemispherical chamber. This experimental work was aimed at checking the results of the computations and to obtain an estimate of the losses, as the numerical code is based on an inviscid, adiabatic flow field.

As it will be seen, the agreement between experimental and computed results was found to be poor. The reasons for these differences are shown to result from computational limitations and recommendations for future work on this subject are given. The actual measured large shock wave attenuation (for example, using a 600 psi $2H_2 + O_2$ driver and a 5/16 inch diameter channel the shock Mach number decreases $M_s \sim 40$ to $M_s \sim 10$ in 70 inches or $\Delta M_s = 5/ft$, see Fig.21) can be attributed to viscous effects primarily, and will be investigated in greater detail. The 5/16 inch diameter barrel is not a realistic shock-tube channel. As noted, it was used to check the limiting case of a massless projectile. In future, 1 inch diameter channels will also be utilized for this study.

2. THEORETICAL CONSIDERATIONS

In this section, a complete description of the program that has been used in this study and its theoretical background are given. This code was developed independently by Piacesi [4] and Sevray [2]. It has been used by Sevray to analyze the operation of the UTIAS Hypervelocity Launcher and to optimize its performance. It was also used with some modifications by Flagg [3] in order to design a second generation launcher, UTIAS Implosion-Driven Hypervelocity Launcher -- Mark II. Although these calculations have been very useful in predicting the analytical performance of the launcher, the actual experimental performance is only of the order of 40% of the computed performance, consequently, it will be necessary to take account of the effects of radiative, convective, ablative and frictional losses to make the calculations more realistic.

For the present work, the code has been adopted to handle the shock tube

case essentially by adding a third region (Fig.2) in front of the diaphragm or of the projectile, which also permits one to analyze theoretically the influence of counterpressure on the velocity of the projectile.

2.1 Description of the Code

This numerical code, written in a Lagrangian form, is based upon the artificial viscosity technique as established by von Neumann and Richtmyer [5] to handle shock-wave problems.

The system (Fig.2) is divided into three regions: the explosive PETN, the gas mixture $2H_2 + O_2$ and air, each having its own equation of state. Each region is further divided into zones and mass points, containing one half the mass of two adjacent zones are assumed to be at the interface of these zones.

2.1.1 Artificial Viscosity Technique

The artificial viscosity is a convenience first introduced by von Neumann and Richtmyer for the numerical treatment of shock waves. Its effect is similar to the effect of a real viscosity. It spreads a shock over a specified number of zones and thus permits one to avoid the treatment of discontinuities running through discrete mass points, which presents serious difficulties in a finite-difference scheme. The spread of the shock can be chosen and held small by the use of proper constants. With the constants used in the present calculations, the shock is actually spread over about 3 zones. The artificial viscosity is restricted to a region which is being compressed and is zero elsewhere. The original form proposed by von Neumann and Richtmyer was:

$$Q = - \frac{(c\rho_o \Delta x)^2}{V} \cdot \frac{\partial V}{\partial t} \left| \frac{\partial V}{\partial t} \right| \qquad (1)$$

with

ρ_o = initial density

V = specific volume

Δx = Zone width

C = constant, determining the spread of the shock

or its equivalent form

$$Q = - \frac{C^2}{V} (\Delta x)^2 \frac{\partial u}{\partial x} \left| \frac{\partial u}{\partial x} \right| \qquad (2)$$

which is valid only for the planar case, where, u is the flow velocity.

Brode [6] proposed a more general form:

$$Q = \frac{C^2(\Delta m)^2}{2VR^{2(\delta-1)}} \frac{\partial V}{\partial t} \left[\frac{\partial V}{\partial t} - \left| \frac{\partial V}{\partial t} \right| \right] \qquad (3)$$

where, $\delta = 1$ for a planer case, $\delta = 2$ for a cylindrical case and $\delta = 3$ for a

spherical case; R is the distance from the origin and Δm is the mass (per steradian, mass/4π for $\delta = 3$; mass per radian unit length, mass/$2\pi \ell$ for $\delta = 2$; mass per unit area, mass/ℓ^2 for $\delta = 1$). Brode's relation depends on the geometry. Wilkins [7], on the other hand, gives the form corresponding to $\delta = 1$ as valid for the three geometries. This simpler form was used since a different form of artificial viscosity in the chamber and in the barrel might lead to difficulties, as one zone can be half in the chamber and half in the barrel.

However, the use of the artificial viscosity techniques may be strongly criticized as it is applied in the region near the origin. In a spherical geometry, this technique is valid only as long as the shock thickness is small compared with the radius of the shock and this is not the case near the origin. From numerous check calculations (Figs. 3 and 4) it is shown that in the zone located at the origin, the pressure due to artificial viscosity (Q) takes on values much larger (up to about 10 times in some cases) than the flow pressure calculated from the equation of state.

Normally, in a planer moving shock wave Q will be of the order of P. In the center of the shock near the origin an additional compression due to the geometry change and the process of reflection takes place, and consequently Q will take on much higher values. It is in this region where the total pressure (P + Q) is largely due to the contribution of the artificial viscosity, that doubts arise whether the computation by using (P + Q) will give a reasonable approximation of the correct pressure history that will act as the driving pressure for the shock or on the projectible inside the barrel. A more detailed study of the Q-method near the origin would be useful and should be done.

This does not seem to affect the x-t diagram of the reflection of the imploding shock, but in all cases leads to erroneous values of the pressure at the origin and consequently it will have some influence on the Mach number of the shock, or on the velocity of the projectile in the barrel. For example, from Fig.3 at $x = 5$ cm, and $t = 45.29$ μ sec, $P = 200$ bars whereas $P + Q = 680$ bars, that is, the artificial viscosity pressure is over twice the actual pressure. Consequently, the equations of motion will be affected. The detailed plot shown in Fig.3, indicates that in the range $50.5 \leq t \leq 58.0$ μ sec, $Q \gtrsim P$. Consequently, errors proportional to the magnitude of Q compared with the true driving pressure, P, can be expected.

2.1.2 Mathematical Formulation of the Problem

This problem can be described in a Lagrangian form by a set of non-linear partial differential equations expressing the equations of mass, momentum and energy, as follows (Ref.6):

Mass: $$V = \frac{1}{\rho} = \frac{1}{\delta} \frac{\partial R^{\delta}}{\partial m} \quad (\delta = 1,2,3) \tag{4}$$

Momentum: $$\frac{\partial U}{\partial t} = - A \frac{\partial (P+Q)}{\partial m} \tag{5}$$

Energy: $$\frac{\partial E}{\partial t} = - (P+Q) \frac{\partial V}{\partial t} \tag{6}$$

Equations of state:
$$\begin{cases} E = E(P,V) \text{ for gas mixture } 2H_2 + O_2 \\ P = P(E,V) \text{ for explosive PETN} \\ E = E(P,V) \text{ for air} \end{cases} \qquad (7)$$

The artificial-viscosity pressure, is restricted to compression only and is expressed as:

$$Q = \frac{(C\,\Delta x)^2}{V}\left(\frac{\partial U}{\partial x}\right)^2 \qquad \text{if } \frac{\partial U}{\partial x} < 0 \qquad (8)$$

$$Q = 0 \qquad \text{if } \frac{\partial U}{\partial x} \geq 0 \qquad (9)$$

where C is a constant which determines the spreading of the shock and is taken as C = 1 for gases, hydrogen-oxygen mixture and air, and C = $\sqrt{1.5}$ for explosive PETN, which corresponds approximately to a spreading of 3 zones.

This set of non-linear, partial differential equations is then transformed into a set of finite differences equations. The two independent variables, time and distance are represented by N and J, corresponding to the number of the cycle being calculated and the label assigned to a mass point. The equations become:

Conservation of mass is assured since we chose a fixed number of mass points.

Momentum:
$$\frac{DU}{Dr} = \left[(P+Q)_{J-\frac{1}{2}} - (P+Q)_{J+\frac{1}{2}} \right] \frac{A_J^N}{\frac{1}{2}\left[m_{J-\frac{1}{2}} + m_{J+\frac{1}{2}}\right]} \qquad (10)$$

Energy:
$$E_{J-\frac{1}{2}}^{N+1} = E_{J-\frac{1}{2}}^{N} - \left[\left(\frac{1}{2} \left(P_{J-\frac{1}{2}}^{N} + P_{J-\frac{1}{2}}^{N+1} \right) + Q_{J-\frac{1}{2}}^{N+\frac{1}{2}} \right] \left[V_{J-\frac{1}{2}}^{N+1} - V_{J-\frac{1}{2}}^{N} \right] \right. \qquad (11)$$

State:
$$E_{J-\frac{1}{2}}^{N} = E\left(P_{J-\frac{1}{2}}^{N}, V_{J-\frac{1}{2}}^{N}\right) \text{ for gas mixture } 2H_2 + O_2 \text{ or air}$$

$$P_{J-\frac{1}{2}}^{N} = P\left(E_{J-\frac{1}{2}}^{N}, V_{J-\frac{1}{2}}^{N}\right) \text{ for explosive PETN} \qquad (12)$$

Artificial viscosity:
$$Q_{J-\frac{1}{2}}^{N+\frac{1}{2}} = C' \frac{\left[U_J^{N+\frac{1}{2}} - U_{J-1}^{N+\frac{1}{2}}\right]^2}{\left[V_{J-\frac{1}{2}}^{N} + V_{J-\frac{1}{2}}^{N+1}\right]} \times \frac{\rho_o}{2} \qquad \text{if } U_J < U_{J-1} \qquad (13)$$

$$Q_{J-\frac{1}{2}}^{N+\frac{1}{2}} = 0 \qquad \text{if } U_J \geq U_{J-1}$$

A^n represents the area of a particular interface, where $\frac{du}{dt}$ is the acceleration of that interface. The constant C^1 in the artificial viscosity is labelled CQSQX in the computer program (Appendix B) and is related to C, the usual constant, as $C^1 = C^2/4$ and m_J is the mass of zone J. We note further that the specific volume V in the computer program is normalized with respect to the initial density.

It should be noted that this condition based on U to determine if a zone is being compressed is only valid in a one-dimensional calculation and should be replaced by a condition based on the specific volume which is valid in all geometries (see equation 3). The solution is then obtained by a stepwise progression in time from the acceleration of an interface based on the old value of the pressure. The new velocity and position of the interface can be calculated. A new specific volume can then be calculated and finally a simultaneous solution of the energy equation and the equation of state yields the new pressure and energy. The calculation can now be repeated for the next time step, etc. Appendix B gives a complete listing and a flow chart of this code.

2.1.3 Stability Requirements

The finite differences schemes are subject to mathematical restrictions which limit the size of time increments that can be taken without the appearance of instabilities. In the actual problem, we have two stability conditions:

a) Courant Condition: This condition, which is very general, states only that the time increment Δt must be small enough that sound signals from one mass point will not have time to reach the next mass point during this time step,

$$\Delta t < \frac{\Delta x}{c} \qquad (14)$$

where, c is the speed of sound in the zone and Δx its length. Appendix A gives the detailed relations used for the calculation of the speed of sound in the various regions.

b) Artificial Viscosity Condition: In the region of compression, where the artificial-viscosity pressure has a value, the form of the differential equations changes from a wave equation to a diffusion type equation. It is shown in Ref.6 that two successive time steps must obey the following relation:

$$\frac{2C\left[V^N_{J-\frac{1}{2}} - V^{N+1}_{J-\frac{1}{2}}\right]}{V^N_{J-\frac{1}{2}}} \cdot \frac{\Delta t^{N+\frac{1}{2}}}{\Delta t^{N-\frac{1}{2}}} \leq 1 \qquad (15)$$

2.2 Problem of Zoning:

The problem of zoning was previously found [2] as one of the most important difficulties of this code and has not yet been solved completely satisfactorily, as a compromise is necessary between the length of computing time, and the precision required. This problem involves in fact a lot of other side problems: the transition between the hemispherical geometry of the chamber and the planar geometry of the barrel; the expansion of the zones as they enter the barrel resulting in extremely long zones; the computing time which already approaches

10 minutes on the IBM 7094 computer in most calculations for the shock tube case. Any refinement in zoning will increase this time considerably.

2.2.1 Initial Zoning

We shall first review the requirements for proper zoning. Proper zoning must lead to a solution of the finite differences equations which is stable and without oscillations in the values of the different physical variables. This solution must be independent of the number of zones used in the computation or at least lead to asymptotic values as the number of zones is increased This asymptotic solution should be obtained with a reasonable number of zones in order to limit the computing time. Finally, this solution should provide a proper description of the phenomena, particularly of the flow in the barrel. This effect on the propagation of a shock has been studied recently with this code by changing the initial zoning which will help us to understand how to choose a proper zoning scheme.

As a shock meets a noticeable increase in zone mass, some peculiar effects occur (see for example the oscillations in the trajectory at t = 13 μsec and t = 24 μsec in Fig.5). The heavier mass point is slow to accelerate and this causes an increase in the pressure of the zone located just behind it. This high pressure now accelerates it too fast, thus causing a decrease in the pressure of this zone and a decrease in the velocity of the mass point. Finally the trajectory of the mass point is oscillating around an average line and the same happens to the shock. For an important increase in zone mass, the shock even reflects clearly on the heavier zone; a weak shock is reflected and a strong one is transmitted. If this zone mass were still increased further, the reflected shock would become the strongest, the transmitted shock would become smaller and even, as a limiting case, disappear for an infinite mass which is equivalent to a solid wall. If we had a large decrease in zone mass, a strong shock would be transmitted and a rare-faction wave reflected. As the imploding shock wave reflects from the origin, these phenomena occur and they cause the oscillations in the calculated pressure. In analyzing the different possible types of zoning, we shall keep in mind these requirements and compare how well these zoning schemes fulfil them.

a) Constant Width Zoning: In a planar, one-dimensional code, constant width zones, which are in that case equivalent to constant mass zones are generally used with success. The first version of this code, which was adapted by Piacesi [8] from a planer code, also divided the various regions into equal width zones. This gave large oscillations in pressure at the time of implosion, as well as unacceptable differences in performance as various numbers of zones were used [2]. A constant width zoning leads to large differences between the mass of adjacent zones and this is the reason for the oscillations which appear in the pressure profile around the implosion. The constant width zoning where the mass ratio of the two zones nearest to the origin is equal to 8 was then abandoned and replaced by an equal mass zoning.

b) Constant Mass Zoning: This type of zoning is without any doubt the optimum one, relative to the disturbances. It gives no oscillations in pressure profiles, no spurious shocks reflected from a change in zone mass. But, due to the size of the zone nearest to the origin (now much larger if the same total number of zones is used: 400 times heavier if 20 zones are used), it results in a lack of detail as to what is happening in the barrel and consequently

results in a dispersion of the final velocity of the projectile for various numbers of zones. There were then two ways to overcome that difficulty, either to increase the total number of zones at the expense of the computing time, or try another type of zoning. To increase the number of zones was judged impractical, since the computing time is almost proportional to the square of the number of zones.

c) Sevray's Zoning: Sevray [2] devised a new zoning scheme in which he tried to keep the main features of a constant mass zoning. He divided the gas regions in three subregions, each being divided into constant mass zones. The subregion nearest to the origin has smaller mass zones. This zoning provides sufficient detail on gas outflow into the barrel and consequently reduces to a reasonable value the dispersion in the final velocity results as different numbers of zones are used (Fig.6). This zoning has been used in the calculation of the performance of the UTIAS hypervelocity launcher by Sevray [2], and in most of the calculations of this report. It is seen from Fig.6 that although the details of the projectile velocity in the barrel differ as the number of zones are increased, the final muzzle velocity at x = 160 cm, is close to 14 Km/sec.

d) Flagg's Zoning: Later, Flagg [3], considering that the differences in mass from one subregion to the next one would introduce spurious shocks and expansions, developed a new partition of zone masses, which is based on the relation

$$\Delta x_j = b_g \frac{j^3 + (n-j)^3}{\sum_{i=1}^{n} i^3 + (n-i)^3} \qquad (16)$$

where b_g is the width of the gas region, Δx_j the width of the jth zone and n the number of zones in this region.

This type of division first appeared to have many advantages and was then used in the calculations of the 30 inch diameter launcher[3] chamber. With the same total number of zones, the mass of the zone nearest to the origin is approximately 10 times smaller than the mass of the same zone in Sevray's calculation, but still 10 times bigger than in a constant width division. It is thus providing a very reasonable detail of the flow in the barrel without slowing down the calculations too much. However, recent investigations have shown oscillations in the pressure profiles as well as unreasonably large differences from the results obtained by Sevray, particularly in the time scale of the events. These oscillations, important mainly at the time of the implosion occur once again because adjacent zones have very large difference in mass. With the zoning of Sevray, if we have 20 zones in the gas, the 5 zones near the origin are of the same mass; with the same number of zones in Flagg's case, these zones vary relatively to the corresponding mass in Sevray s case as 0.10, 0.63, 1.08, 1.55 and 1.85 (a factor of 6 between the two first zones, a factor of 18 in the 5 first zones). With this zoning, as the number of zones is increased, the time of implosion comes near to the value found in Sevray's calculations. (That is the time to implosion is increased owing to the cumulative propagation time between zones). However, at the same time the instabilities in the pressure profiles are very much increased, as shown on

Fig.7 where the same case (30 inch diameter chamber, 12.65 g projectile, 25 kg of PETN and 200 psi $2H_2 + O_2$) is represented with different zoning schemes. This increase in instabilities can be easily explained. The mass ratio of the two zones closest to the origin can be expressed as

$$\frac{M_n - 1}{M_n} = \frac{v_n - 1}{v_n} = \left[\frac{\Delta x_n + \Delta x_n - 1}{\Delta x_n} \right]^3 = \left[1 + \frac{\Delta x_n - 1}{\Delta x_n} \right]^3 = \left[1 + \frac{(n-1)^3 + 1}{n^3} \right]^3 \qquad (17)$$

An examination of this ratio shows that it is an increasing function of n for $n > 2$ varying between 1.95 as $n = 2$, and 8 as n goes to infinity.

Despite the advantages of this zoning, to obtain a detailed description of the outflow in the barrel, this type of zoning has to be abandoned as we do not know the influence of the oscillations in the pressure at the origin on the final velocity and cannot tolerate such variations on the time of the implosion.

Another zoning scheme, similar in principle to the one used by Sevray, has also been developed in order to have smaller zones around the origin. The gas region is now divided into 7 subregions, each being divided into the same number of zones. Between each subregion there is a mass ratio of the order of 2. This permits one to have zones around the origin of the same size as the central zone in Flagg's zoning, but the fact that the change in mass is smaller and also far from the origin prevents the oscillations. This zoning scheme will be used further to show the influence of the mass located at the origin on the velocity profile of a shock wave propagating along the barrel.

2.2.2 Transition Between Spherical and Planar Geometry

The treatment of the origin region, i.e., of the transition between the spherical geometry existing in the chamber and the planar geometry in the barrel becomes a more and more important factor as the zoning scheme used give smaller zones around the origin. When the zoning of Sevray is used, we have only one or two zones located at the same time in the transition region; with the finer zoning, previously described, we may have up to about 10 zones in this region. More care must then be taken how to realize a smooth transition from the spherical to the planar flow and the approximate treatment of Sevray is no longer acceptable in such a case.

It is important to note that this transition is clearly a two-dimensional phenomenon and a more complex type of code should really be used and there is no way to treat it rigorously with a one-dimensional code. Some approximations have to be made in order to realize this transition in a manner which does not seriously affect the flow.

In the first version of the code, the flow is considered as hemispherical upstream from the origin and planar downstream. This led to many difficulties and disturbances as shown previously in Ref.2 and was then abandoned. Sevray made this transition in two discontinuous steps for the area (Fig.8) but kept the old routine for the calculation of the specific volume. This is

without consequence as long as only one or two zones are in the transition region but if more are inside, it must be avoided and a smooth transition must be adopted.

Later Flagg [3] developed a continuous transition, taking the area as the one of a spherical segment supported by the barrel circumference and the volumes as defined by these surfaces. This transition treatment is much superior to Sevray's treatment, for it is continuous, but it must be noted that many other continuous transitions could have been developed and used as well. All these solutions have no real physical meaning and are somewhat arbitrary, but the treatment of a two-dimensional phenomenon with a one-dimensional code can be nothing but approximate and only a two-dimensional code can treat it rigorously. This problem is presently being considered at UTIAS.

2.2.3 Redivision of Long Zones in the Barrel

The barrel is of a very small diameter, so that for any reasonable number of zones, one zone as it expands can occupy a very long distance in the barrel, thus providing insufficient detail on what is happening in the barrel. To overcome this problem, Sevray introduced a scheme to split the zone next to the projectile in two zones of equal mass and pressure, whenever its length was greater than 3 cm. This scheme was approximate and worked very well as long as a projectile case was calculated. Later, as the shock-tube cases were run, it led to very big disturbances and another scheme had to be found.

To explain why this happened, let us consider the momentum equation for the projectile:

$$\frac{dU}{dt} = \left[(P+Q)_{J-\frac{1}{2}} - (P+Q)_{J+\frac{1}{2}} \right] \frac{A_J^N}{\frac{1}{2} m_{J-\frac{1}{2}} + m_{proj} + \frac{1}{2} m_{J+\frac{1}{2}}} \qquad (18)$$

In the denominator of this expression, $m_{proj.}$ is the most important term and the division by 2 of $m_{j-\frac{1}{2}}$, as the zone is divided, has no serious influence on the acceleration of the projectile. However, if we now consider a shock tube case and look again at the denominator of this expression applied at the interface, we note that, $m_{proj.}$ being equal to zero and $m_{j+\frac{1}{2}}$ being very small, owing to the low pressure in the channel, $m_{j+\frac{1}{2}}$ becomes the most important term, so that dividing $m_{j-\frac{1}{2}}$ by 2 is almost equivalent to multiplying the acceleration of this interface by 2, thus leading to the disturbances we found. Even if these disturbances damp out, what their actual influence on the result maybe is difficult to evaluate and it is preferable to avoid them.

Another scheme based on a more realistic hypothesis was developed. It permits a split of any zone in the barrel into two zones of equal mass (and not only the zone placed just behind the interface) whenever its length increases too much. Essentially, this scheme keeps constant the values of the acceleration on both boundaries of the zone which will be divided, and that permits one to assign to each new zone a pressure calculated from the momentum equation. The specific volumes, rather than being taken equal in both zones, are now calculated from the pressure assuming a γ law relation between pressure and density and an effective γ equal to 1.14 as mentioned by Flagg [9]. The energy is then calculated from pressure and density using the equation of state, and the conservation of

energy gives the kinetic energy of the new mass point and thus its velocity. This procedure permitted one to obtain a much better description of the flow in the barrel, but in consideration of the other limitations of the code and of the increase in computing time, it was used only in a small number of cases to check its influence. This influence was found to be not important and justifies the fact that it was not used regularly in the calculations.

2.3 Equations of State

Another major difficulty of such calculations is to find appropriate equations of state for the different materials involved, particularly when the conditions are extreme as they are in our case where the pressure and temperature at the origin are ideally infinite at the time of implosion. The three equations of state that were used are real gas equations of state, but have been used well beyond their range of applicability.

2.3.1 Equation of State of the Gas Mixture $2H_2 + O_2$

It is an extrapolation of the real gas calculation of Moffatt [10] done by Brode and programmed by Piacesi. It is expressed as

$$E = 6.57 \times PV + \frac{974.0\,(PV)^2}{1140.0 + (PV)^4} - \alpha \left[0.101\times10^{-3} \mathrm{Ln} \frac{P}{1.013\times10^{3}} - 0.2325\times10^{-3} \right] \qquad (19)$$

where:

$\alpha = 0$ for $PV \leq 1.0465$

$\alpha = 8600\,PV - 9000$ for $1.0465 < PV \leq 3.488$

$\alpha = 21\times10^{3}$ for $3.488 < PV$

the units are:

P in 10^{10} erg/cc = 10^{4} bars

E in 10^{10} erg/g = 10^{4} bar-cc/g.

V in cc/g.

This equation is representative of the $2H_2 + O_2$ mixture in the range:

$1600^{\circ}\,K < T < 6000^{\circ}\,K$

$0.01\ \text{bar} < P < 1000\ \text{bars}$

and has been used well beyond these limits in our calculations, since unfortunately no calculations are available for a stoichiometric mixture of hydrogen-oxygen for temperatures to $10^{6}\,^{\circ}K$ and pressure of the order of 10^{5} bars. However, it has been shown that at high pressure this equation of state is closely equivalent to a flow with $\gamma = 1.14$, which is in good agreement with other

available calculations [11].

2.3.2 Equation of State for the Explosive

This equation is a numerical fit to the experimental data of a 50% mixture of PETN and TNT (pentolite) provided and programmed by Piacesi. It is written as

$$P(E, V) = A_{(\rho)} + B_{(\rho)} E \qquad (20)$$

where

$$A = 0.002164\rho^4 + 2.0755e^{-6.0/\rho}$$

$$B = 0.35\rho$$

$$\rho = \frac{\rho_o}{V}$$

ρ_o is the initial density and was taken as $\rho_o = 0.58$ g/cc. The units are:

P in megabars

E in megabar - cc/g

It must be mentioned that both the equation of state for the gas and the equation of state for the explosive do not give directly the temperature and in this code we deduce it from the ideal relation PV = RT where, R = $\mathcal{R}$/M and M, the molecular weight. The molecular weight of the mixture varies with the degrees of dissociation and ionization and is thus a function of the temperature. For the $2H_2 + O_2$ mixture, M was taken as 12 which corresponds to the unreacted mixture. For the explosive, M was taken as 1, since we did not know the composition of the products of detonation of pentolite and corrections have to be made to obtain a reasonable value of the temperature. The temperatures are thus inaccurate and give only some indications of their variations with time or position. It is hoped that better calculated temperatures will be obtained in future calculations, at UTIAS.

2.3.3 Equation of State for Air

First a perfect gas equation PV = RT was used, but later it was found a more accurate equation would be preferable. An equation of state was then programmed from an extrapolation of the calculations of Gilmore [12] done by Brode [13].

A convenient form to write this equation of state for air is

$$\theta = \zeta S(\zeta)$$

$$\zeta = \frac{\pi}{\tau_1}$$

$$\epsilon = \frac{\gamma_o - 1}{2} \zeta (\mu - 1) \qquad (21)$$

$$\mu = \mu(\zeta, \tau_1)$$

$$\xi = \mathrm{Ln}(\tau_1)$$

with the non-dimensionalized variables

$$\pi = \frac{P}{P_o} \quad \text{with} \quad P_o = 1 \text{ atm.}$$

$$\eta = \frac{\rho}{\rho_o} \quad \text{with} \quad \rho_o = 1.293\ 10^{-3} \text{ g/cc.}$$

$$\epsilon = \frac{E}{E_o} \quad \text{with } E_o = 1960.\ 0 \text{ bar-cc/g.}$$

$$\theta = \frac{T}{T_o} \quad \text{with } T_o = 273.92\ ^{o}\text{K.}$$

we have

$$S(\zeta) = \frac{485}{1000 + \zeta^2} + \frac{3860}{7500 + 26.5\zeta} \tag{22}$$

$$\mu = \mu_o + 0.09\ (\mu_o - \mu_2)\ \xi \tag{23}$$

taking $y = 1/\xi$, μ_o and μ_2 are given by the following relations

$$\mu_o = 1 + \frac{25.894868\ y+3}{4.778973\ y+1} + \frac{860\ y(1-y)}{3000\ y^2+1} + \frac{2536\ y(1-y)}{9\ 10^4\ y^2+1} + \frac{41000\ y(1-y)}{12\ 10^6\ y^2+1} \tag{24}$$

$$\mu_2 = \frac{6002\ y + 4}{1000\ y + 1} \tag{25}$$

this equation of state is valid for temperatures up to 24,000 ^{o}K and was used almost only in its range of validity.

2.4 Detonation Scheme

In programming the equations of state for explosive and for gas mixture $2H_2 + O_2$ the detonation scheme described by Wilkins [14] was used. In each zone, the burn fraction F defined as

$$F = \frac{1 - V}{1 - V_{cj}} \tag{26}$$

is calculated and the pressure in the zone is defined as

$$P = P\ (E,\ V)\ x\ F \tag{27}$$

where, V is the specific volume and V_{cj} the Chapman-Jouguet volume. This burn fraction F is used to spread the detonation front over several zones in the same manner as the artificial viscosity spreads a shock front over several zones. The burn calculation is started by setting F = 1 in the zone that

corresponds to the point of initiation of the detonation. When F = 1 for a zone, then all the chemical energy contained in that zone has been deposited and F remains equal to 1 thereafter.

It should be noted that the calculations will proceed over several zones (Wilkins [7] mentions 2 to 3 times the number of zones on which the artificial viscosity is spread over, i.e., 15 zones approximately in our problem, but calculations seem to show a much smaller number) before the detonation front is correctly established. This implies the use of a maximum number of zones in order to obtain reasonable accuracy in the detonation velocity and consequently in the time scale of the phenomenon. The Chapman-Jouguet volumes which were used in this work are

$$V_{cj}\ (\text{PETN}) = 0.7872 \qquad (28)$$

$$V_{cj}\ (2H_2 + O_2) = 0.54$$

In previous works [2-3], unfortunately an erroneous value of the Chapman-Jouguet volume for PETN has been used. Some runs have been done to check the influence of this parameter and it was found this error did not affect the results seriously as shown in Figs. 9 and 10. It is seen that the correct value ($V_{CJ} = 0.7872$) gives a higher (4%) final contact surface velocity and lower implosion pressure at the origin.

3. RESULTS OF THE COMPUTATIONS:

Only a few results indicative of the general trend will be given in this report since it has been recently found following a comparison with experimental results, that they were of limited value. In Section 5, the reasons for this fact will be explained in detail and some indications of the remedy that could be applied to improve these calculations and make them more reliable will be given.

3.1 The Shock Tube as a Limiting Case of a Hypervelocity Launcher as the Mass of the Projectile Goes to Zero

The case presented consists of an explosive loading of 100 g PETN, an initial pressure in the chamber of 400 PSIA $2H_2 + O_2$ and an air pressure of 1 torr in the barrel. Four runs were made with the mass of the projectile varying: 1.72 g, 1.0 g, 0.5g and 0.2 g. The results are shown on Figures 11 and 12. Figure 11 indicates the variation of the velocity of the projectile or interface at 2 meters as the mass of the projectile decreases and goes to zero. On Figure 12 is given the variation of the velocity profile at a distance of two meters from the origin with the mass of the projectile as a parameter.

From Figure 11 it can be seen that as the mass of the projectile decreases, the importance of the first peak pressure on the base of the projectile becomes bigger and finally as the mass decreases still more, the influence of the second peak disappears completely. The trajectory of the projectile is now determined by the first implosion and shock waves in the barrel generated by the following implosions will no longer overtake it. Figure 12 shows that as expected the projectile velocity increases with decreasing mass. It was not possible to go to masses $m < 0.2$ g, as the program

[illegible] only unable to give a solution for small masses. This is unfortunate as it would yield the shock tube case. The entire numerical program is presently under review.

3.2 Shock Tube Calculation

3.2.1 Gas Case:

Results were obtained for gas cases with an initial pressure in the chamber of 200, 400, 600, 800 PSIA $2H_2 + O_2$. Figure 13 gives the different velocity profiles obtained. It is seen they are very similar and the velocities of the interfaces differ only slightly. This is not physically realistic for we can expect a considerable increase with initial driving pressure especially near the origin, before attenuation sets in. The fact that no change is observed is indicative of some computational problem. These unexpected computational results coupled with the experimental results show (see Section 6) the inability of this code to describe the phenomenon.

3.2.2 Explosive Case:

A series of runs with the 8 inch diameter chamber and a 5/16 inch diameter barrel has been run for a constant initial pressure of 200 PSIA in the chamber and diverse explosive loading: 100 g, 200 g and 400 g. Figure 14 gives the interface velocity for these diverse cases. It is seen that the final velocity at 10 meters first increases with increasing explosive weight, goes through a maximum and then decreases as the weight of explosive is further increased. This emphasizes the need for an optimization of the initial conditions to obtain the highest Mach number (see Ref.2). However, in the light of the comparison between computed and experimental results, this optimization has not been completed using the present program.

Figure 15 is the time-distance diagram of a shock tube case with an explosive loading of 200 g PETN and an initial pressure of 200 PSIA $2H_2 + O_2$ for a 5/16 inch diameter channel. The successive implosions were followed and it is interesting to remark that the successive shocks they generate in the barrel propagate with lower and lower velocity and will never overtake so that the trajectory of the interface is in fact determined only by the first implosion. It is seen that shock Mach numbers, $M_s \sim 100$ may be achieved.

Figure 16 gives the pressure profiles at various instants corresponding to the case shown on Fig.15. It is seen that uniform flow exists between the contact surface and the shock wave. If this result is verified experimentally it would be most encouraging to use the present facility to generate uniform flow regions at extreme temperatures and pressures. Figure 17 shows the influence of counterpressure on the velocity of the interface. There is only a few per cent difference between 0.1 torr and 1 torr. However, the profile changes considerably and inexplicably as the counterpressure is increased to 50 torr. The remarks made in the previous subsection also apply here. It can be seen that during the early phase of the flow the counterpressure has little effect on the accelerating interface velocity. Whereas, in practice, the gas escape speed as obtained from the chamber temperature sets an upper bound near the origin and viscous effects will decay this speed with distance.

4. EXPERIMENTAL RESULTS:

4.1 Equipment

All experimental runs were done in an 8 inch diameter, hemispherical

chamber. The barrel was made of stainless-steel, high-pressure tubing with a 5/16 inch internal diameter and was approximately 4 meters long. Scribed stainless steel diaphragms, 0.015 inch thick, which had been tested previously by Watson [15], were used and chosen following his recommendations.

The velocity of the shock was measured using three different methods:

1) Ionization Gauges: they detect the arrival of the ionization front which accompanies the shock. They were the principal measuring system.

2) Photomultipliers: they detect the arrival of the luminous front which accompanies the shock. They have been used as an independent way of measuring the time of arrival of the shock at a fixed station in order to check the results given by the ionization gauge technique.

3) Microwave: in association with Elsenaar [16], this method should have given a continuous measurement of the velocity of the shock wave and by following the profile it should have been possible to evaluate boundary-layer effects and shock-wave attenuation in the barrel. But unfortunately the reflection of the microwaves from the shock was very weak owing to the low power level of the existing equipment and no practical results could be obtained.

4.2 Ionization Gauges

The ionization gauges consisted of a thin copper wire (1/32 inch diameter) placed in a hole in the wall of the barrel and well insulated from the wall. They extended about 0.5 mm inside the barrel. Over each ionization gauge, the barrel was reinforced with a tight collar to prevent the gauge from leaving its hole as the pressure in the channel increased, following the arrival of a shock. Five ionization gauges were placed along the barrel at fixed intervals of 14 inches. During an experiment, they were charged at 300 volts D.C. To prevent accidental discharge, they were checked before a run at 500 volts D.C. These ionization gauges were connected to a circuit transforming their signals into sharp pulses which were recorded on an oscillograph. We had already at UTIAS one circuit (Fig.18) designed by Flagg [9] for his measurement of the incident detonation wave and reflected shock in the one-dimensional chamber. This circuit had been designed to be able to distinguish shocks at intervals of about 5 μs. This led to difficulties in the first measurements. The same ionization gauge was giving several signals corresponding to the arrival of the different shocks caused by the successive implosions and on the record there was no way to distinguish between them. A new circuit was then designed with a time constant for charging of the order of 150 milliseconds and a time constant for discharging of the order of 2 microseconds. This circuit represented on Fig.18 was built and used with success. The signals attenuated 28.2 times were recorded on a zig-zag (or raster) oscillograph together with the signals of a 10-microseconds time-mark generator. The oscillograph was triggered from the ignition and a time of 76 microseconds was assumed between the ignition and the first implosion.

4.3 Verification of the Ionization Gauge Technique

After the first experiments which showed velocity profiles quite different from the computed profiles, it was decided to check the ionization gauge technique. This was done by placing at the same distance from the

origin an ionization gauge and a photomultiplier looking through a window into the barrel. The window was a 1/16 inch diameter hole, drilled perpendicularly to the barrel and filled with a transparent resin. The time of arrival of the luminous front and of discharge of the ionization gauge were recorded separately as shown on Fig.19 for a 200 PSIA $2H_2 + O_2$ case. The agreement between the two techniques was found to be very good.

4.4 Experimental Results

Only a few cases have been run so far, mainly for two reasons:

1) They showed sufficient evidence that the computations were not adequate.

2) We were strongly limited in our choice of initial conditions by the strength of the hemispherical chamber, which had been previously damaged and could no longer stand explosive runs.

For these reasons only three cases have been run and duplicated in order to obtain average values since the reproductibility was not always very good; initial pressure of these were 200 PSIA, 400 PSIA and 600 PSIA $2H_2 \cdot O_2$ without explosive and with a counterpressure of 1 torr or 10 torr.

Figure 20 gives the oscillograph recordings of a 400 PSIA $2H_2 + O_2$ case. On Fig. 21 the velocity profiles versus distance of the three studied cases are given. Two points, where the velocity of the shock in the 400 PSIA case was measured with the microwave equipment [16] are also given on this previous figure. These points are in good agreement with the ionization gauge measurements. The three profiles have the same general character: very high initial velocity followed by an extremely rapid attenuation of the shock. For example, in the 600 psi $2H_2 + O_2$ case, the shock wave attenuates from $M_s \sim 40$ to $M_s \sim 10$, in 6 ft. This attenuation was first judged too strong, but it is in fact not so strange when we consider such high Mach numbers flow in a pipe of such a small diameter, and we have probably a fully developed pipe flow. Other runs have been done last year by Flagg, with variable explosive loading since at that time the chamber could stand 200 g. PETN. These runs show the same general features but they have been done with only two ionization gauges and consequently give only a rough idea of the velocity of the shock.

More experimental runs will have to be done in order to evaluate completely the possibilities of this device and the influence of radiative, convective, ablative and frictional losses, and to optimize its performance. With the new launcher which has been designed, it will be possible to use a 1 inch diameter barrel and this should permit us in the future to carry out more realistic and useful experiments. However, for the aim of this study, these few runs have been sufficient, permitting us to test well the code used and to show its inability to describe accurately the phenomena occurring in such a shock tube as will be shown subsequently.

5. COMPARISON BETWEEN THEORETICAL AND EXPERIMENTAL RESULTS

Figure 22 shows on the same plot the velocity profile of the shock in a 200 PSIA $2H_2 + O_2$ gas case computed from this code and as measured experimentally. The two profiles are quite different and it was suspected that the ionization gauges were not working properly. However, after the gauges were checked by an

independent technique, the optical measurement of the arrival of the luminous shock front, and after having duplicated all runs and obtained results within 20 per cent it was no longer possible to doubt the results. The calculations were then checked with great care and we arrived at the conclusion that the computer code was unable to describe accurately the starting process of this shock tube.

Let us consider the movement of the interface between the gas mixture $2H_2 + O_2$ in the chamber and the air in the barrel. Just at the time at which the diaphragm breaks. This movement is governed by the momentum equation:

$$\left(\frac{dU}{dt}\right)_J = \frac{A_J^N \left[(P+Q)_{J-\frac{1}{2}} - (P+Q)_{J+\frac{1}{2}}\right]}{\frac{1}{2}\left[m_{J-\frac{1}{2}} + m_{J+\frac{1}{2}}\right]}$$

For a given pressure difference across the interface, the acceleration depends on the values of the masses $M_{j-\frac{1}{2}}$ and $M_{j+\frac{1}{2}}$. In the channel, the pressure is very low, so that the mass $M_{j+\frac{1}{2}}$ is very small: typically, for a pressure of 1 torr and a 5 cm long zone, $M_{j+\frac{1}{2}}$ is equal to $0.4\ 10^{-5}$g. On the other side, $M_{j-\frac{1}{2}}$, the last zone in the gas mixture is in a typical run using Sevray's zoning [2] with 20 zones in the gas of the order of 0.1 g, so that the acceleration of the interface is almost inversely proportional to the mass of this zone. This picture is rigorously true only for the cycle at which the diaphragm will burst, as the breaking pressure has been constantly chosen as 1000 bars. For subsequent cycles, the driving pressure will also be dependent on the mass $M_{j+\frac{1}{2}}$. However, the influence of the value of the mass located at the origin was clearly shown as another type of zoning problem in Sec. 2.2.1. The zoning used allowed us to have a mass at the origin approximately 10 times smaller than with Sevray's zoning, with only 35 zones. Figure 23 shows how the velocity profile varies. As expected from previous consideration, the inital acceleration of the interface is much higher. In addition, the final velocity is much higher. The latter result could not have been predicted beforehand. This can be understood and explained: in the first case, with a heavy mass at the origin, it takes a long time for the interface to attain its final velocity and is still accelerating at 10 meters from the origin, where the calculation was stopped; when a much lighter mass is located at the origin, the interface accelerates much faster and the final velocity is obtained in a much smaller distance. It is interesting to mention that if we apply the theory of a perfect shock tube [17], the initial acceleration of the interface is infinite. From the previous considerations it is seen that to approach such a result we should have $M_{j-\frac{1}{2}}$ of the same order as $M_{j+\frac{1}{2}}$. However, the continuity of the masses across the interface is difficult to obtain and would require an extremely large number of zones.

The results of Section 3.2.1 can now be explained. The shock Mach numbers calculated for initial pressures of 200, 400, 600 and 800 PSIA $2H_2 + O_2$ were found to be almost the same, as shown on Fig. 13, when they should have increased with initial pressure. In the computations when the initial pressure is doubled, the pressure in the chamber is also approximately doubled. However, if we keep the same total number of zones in the gas, the mass of the zone located at the origin is also doubled and both effects compensate in the momentum equation to give the same acceleration.

From the previous discussion, it is seen that,

a) the computed velocity profile is not realistic

b) the velocity obtained at 10 meters is not the final velocity, since the interface is still accelerating

Consequently, the code, as used is inadequate for such calculations. The following improvements may be implemented in order to make the calculations closer to reality.

6. FUTURE WORK

Several changes to the present code will have to be made, but there are three main directions in which improvements will have to be found and these will be reviewed in order of importance.

a) Initial Zoning: As shown in Section 2.2.1 and 5, large discontinuities in zone mass cannot be tolerated and continuity of zone mass must be insured across the interface. From recent discussions with Dr. H. L. Brode [18], it has been concluded that even Sevray's zoning is not acceptable since the ratio of zone masses of two adjacent subregions which is equal to 3 is too big. However, a 10 per cent increase in mass from one zone to the next may be acceptable. This suggests the use in the chamber of zoning in which as we go away from the origin, the zone mass is increased by a fixed percentage of the order of 10 per cent. A reasonable number of zones would have to be assumed in the explosive region and the number of zones in the gas region would be determined by requiring continuity of zone mass through the interface gas mixture $2H_2 + O_2$/air and gas mixture $2H_2 + O_2$/explosive. Such zoning would be ideal. There are no longer any important discontinuities in zone mass and thus spurious shocks or expansions are avoided. The mass located at the origin is now very small and of the same size as the masses in the barrel thus being independent of the pressure in the chamber, and the difficulties explained at the end of Section 5 are avoided. However, such zoning will lead to very large numbers of zones and require extremely large storage of data. The time of computation will be very long and will limit the number of cases that can be run, so that a compromise will probably have to be found. An additional problem is that for very small zones the transition between the spherical and planar geometry (see Sec.2.2.2) becomes extremely important. As noted before, only a two-dimensional treatment of the transition region will describe the local flow accurately.

b) Equations of State: When a more accurate code will have been developed, it will become necessary to use more precise equations of state in order to be able to compare experimental and computed results. The present equations have been used well beyond their limits of validity. This problem is actually under investigation and it is hoped that we will soon have a better equation of state for the mixture $2H_2 + O_2$. The equation of state for the explosive, PETN, will also have to be reconsidered since the equation we use is in fact an equation for pentolite (50 per cent of PETN and of TNT).

c) Artificial Viscosity Technique: The Q-method will have to be investigated much more. The form of the artificial viscosity should be chosen as described by Brode [6] and the criterion presently based on the velocities will have to be replaced by a criterion based on the specific volume. The artificial viscosity technique leads to an erroneous value of pressure in the zone located at the origin and this effect on the final performance will have to be evaluated.

7. CONCLUSIONS

The experimental measurements of shock velocity using ionization gauges have shown that the numerical code used in this work was not very successful in predicting the performance of the UTIAS implosion-driven shock tube. The deficiencies of the code have been analyzed in detail and recommendations have been given to overcome some of these difficulties. The main problem is to choose proper initial zoning that would avoid computational effects and errors arising from a large change in zone mass and which will still not lead to unreasonable computing times.

REFERENCES

1. Glass, I. I. — Shock and Combustion Wave Dynamics in an Implosion-Driven Hypervelocity Launcher, Institute for Aerospace Studies, University of Toronto, Review No.25, 1965, (also ARL Report No. 67-0018)

2. Sevray, P.A.L. — Performance Analysis of UTIAS Implosion-Driven Hypervelocity Launcher, Institute for Aerospace Studies, University of Toronto, Technical Note No.121, 1968. (also ARL Report No. 68-0018).

3. Flagg, R. F.
Mitchell, G. F. — An Optimization Study of the UTIAS MK II Implosion-Driven Hypervelocity Launcher, Institute for Aerospace Studies, University of Toronto, Technical Note No. 1[illegible], 1968.

4. Piacesi, R. — Private Communication.

5. von Neumann, J.
Richtmyer, R. D. — A Method for the Numerical Calculation of Hydrodynamic Shocks, J. Appl. Phy. Vol. 21, p.332, 1950.

6. Brode, H. L.
Asuno, W.
Plemmons, M.
Scantlin, L.
Stevenson, A. — A Program for Calculating Radiation Flow and Hydrodynamic Motion, Rand Corp. Memorandum RM-5187-PR, Santa Monica, California. 1967.

7. Wilkins, M. L. — Calculation of Elastic-Plastic Flow, Methods in Computational Physics, Edit. by Alder, Ferbach and Rotenberg, Academic Press, Vol. 3, 1964.

8. Piacesi, R.
Gates, P. F.
Seigel, A. E. — Computer Analysis of Two Stage Hypervelocity Model Launchers, U. S. Naval Ordnance Laboratory, White Oak, Maryland, NOLTR 62-87, 1962.

9. Flagg, R. F. — The Application of Implosion Wave Dynamics to a Hypervelocity Launcher, Institute for Aerospace Studies, University of Toronto, Report No. 125, 1967. (also ARL Report No. 67-0220).

10. Moffatt, W. G. — The Thermodynamic and Electrical Properties of Dissociated Combustion Gases, Magnetogasdynamic Laboratory Report 61-5, Massachusetts Institute of Technology, 1961.

11. Benoit, A. — Equilibrium Thermodynamic Data for the H_2-O_2 System, Institute for Aerospace Studies, University of Toronto, Technical Note No. 128, 1968.

12. Gilmore, F. R. — Equilibrium Composition and Thermodynamic Properties of Air to 24000° K, Rand Corp. Memorandum RM-1543, Santa Monica, California, 1955.

13. Brode, H. L. — A Calculation of the Blast Wave from a Spherical Charge of TNT, Rand Corp. Memorandum RM-1965, Santa Monica, California, 1957.

14. Wilkins, M. L. — Calcul de detonations mono et bidimensionelles, Colloques Internationaux du Centre National de la Recherche Scientifique sur les ondes de detonation, 1961.

15. Watson, J. D. — Implosion-Driven Hypervelocity Launcher Performance Using Gaseous Detonation Waves, Institute for Aerospace Studies, University of Toronto, Technical Note No. 113, 1967 (also ARL Report 67-0278).

16. Elsenaar, A. — A Microwave Investigation of the Projectile Motion in the Barrel of the UTIAS Implosion-Driven Hypervelocity Launcher, M.A.Sc. Thesis, University of Toronto, (1969).

17. Glass, I. I. — Handbook of Supersonic Aerodynamics, Section 18, Shock Tubes, NAVORD Report 1488, Vol.6, 1953.

18. Brode, H. L. — Private Communication, 1968.

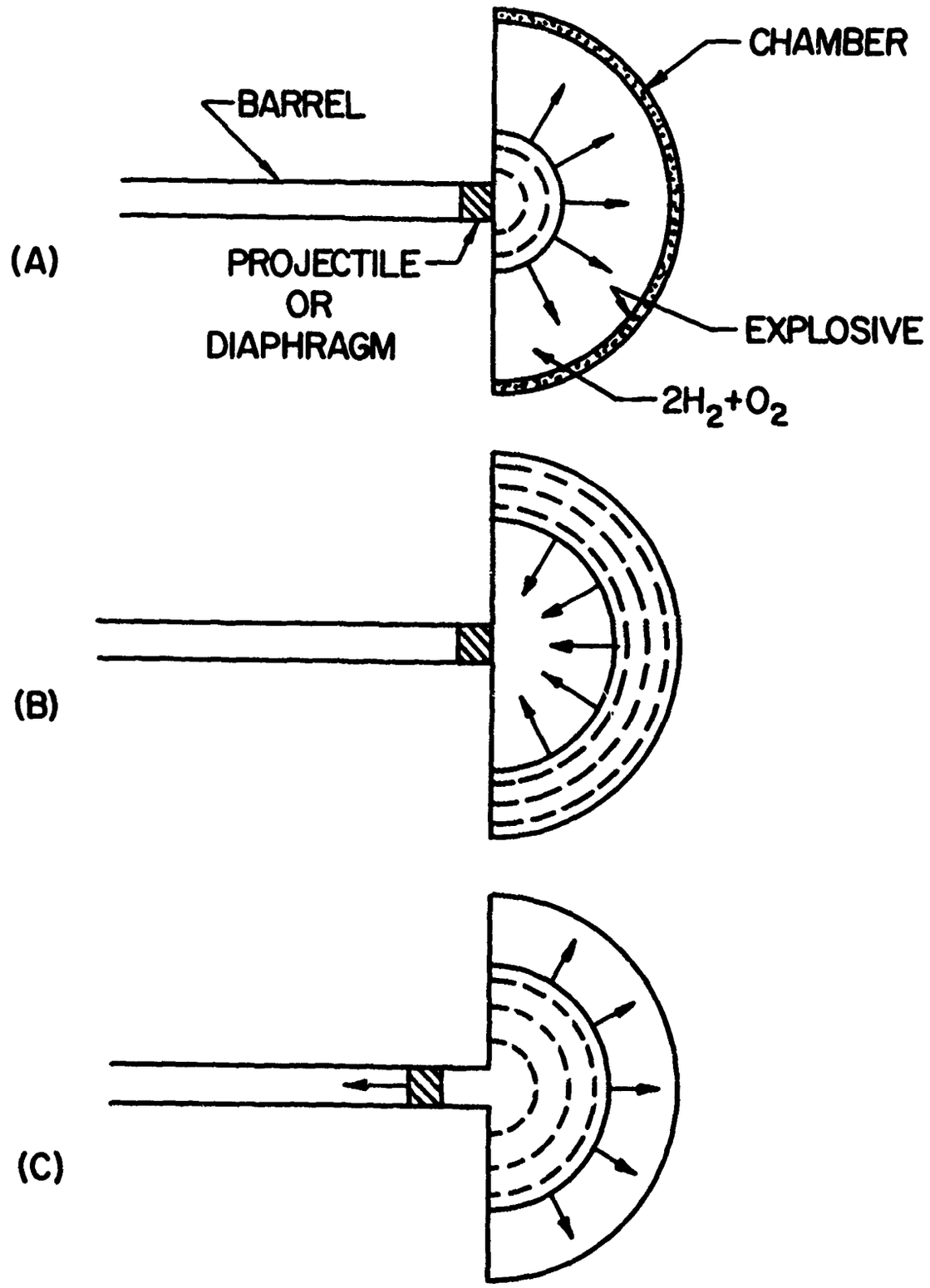

FIG. 1 SCHEMATIC OF PRINCIPLE OF OPERATION OF UTIAS HYPERVELOCITY LAUNCHER

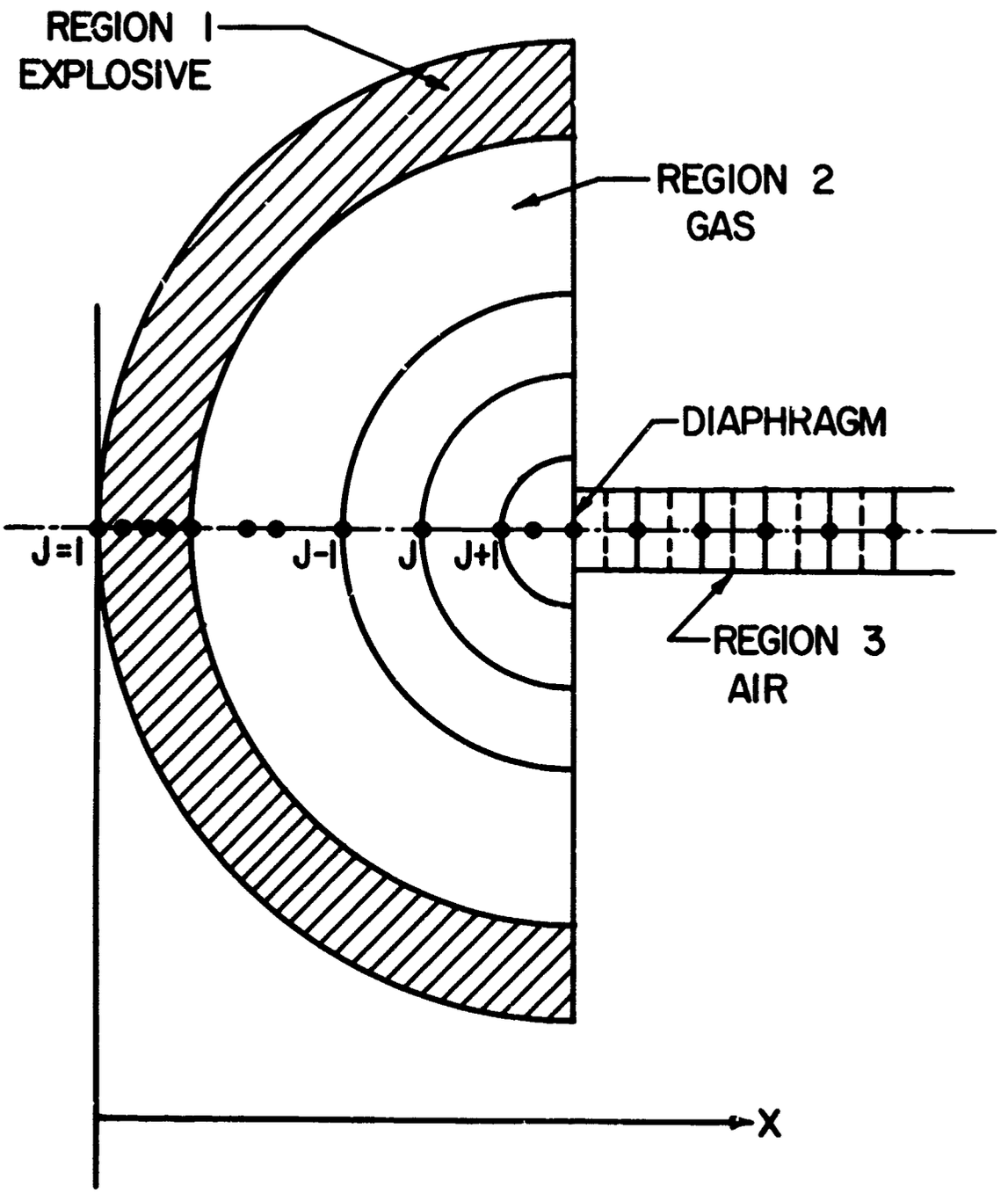

FIG. 2 DISTRIBUTION OF MASS POINTS

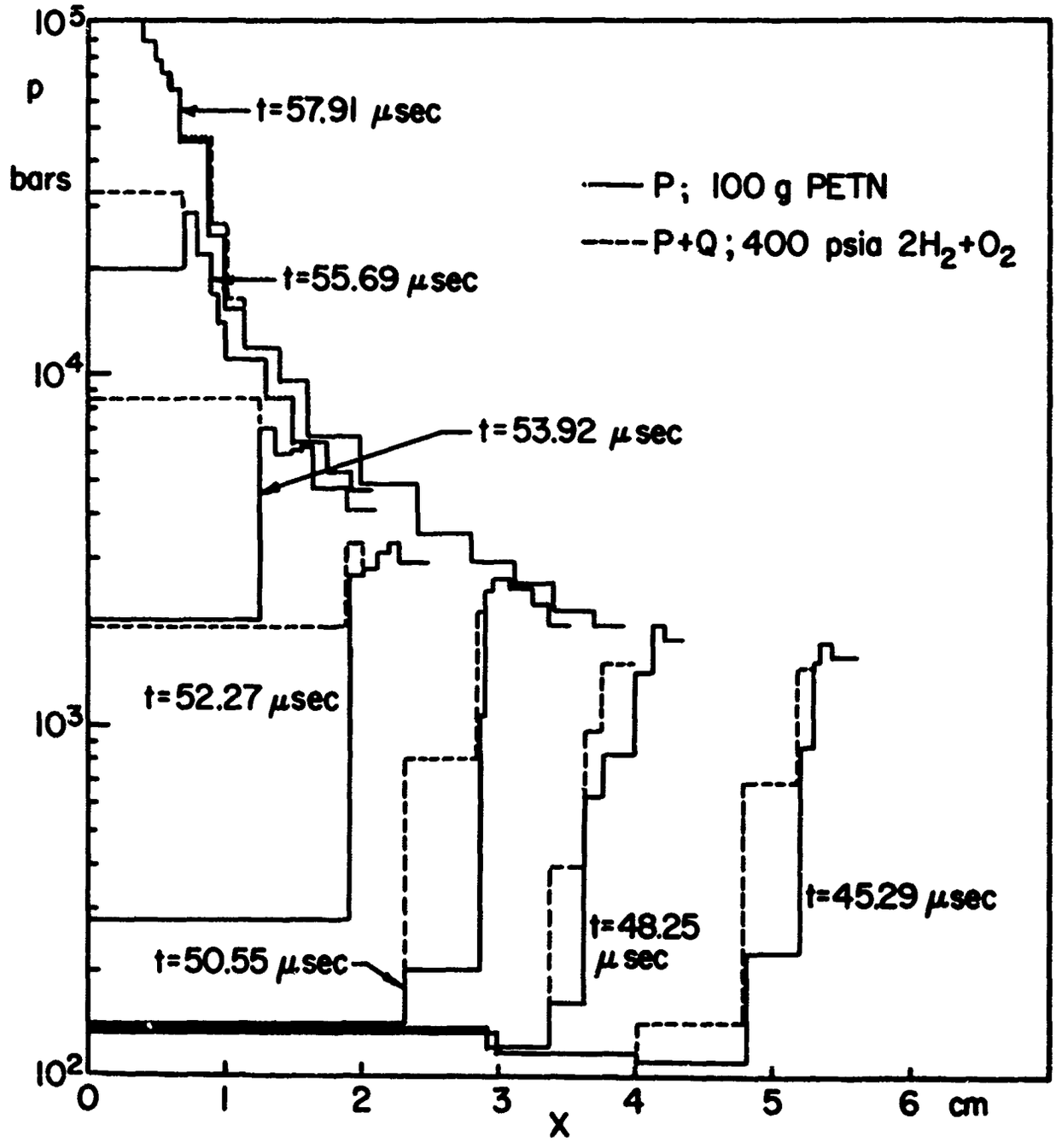

FIG. 3 EVOLUTION OF THE PRESSURE PROFILE NEAR THE IMPLOSION

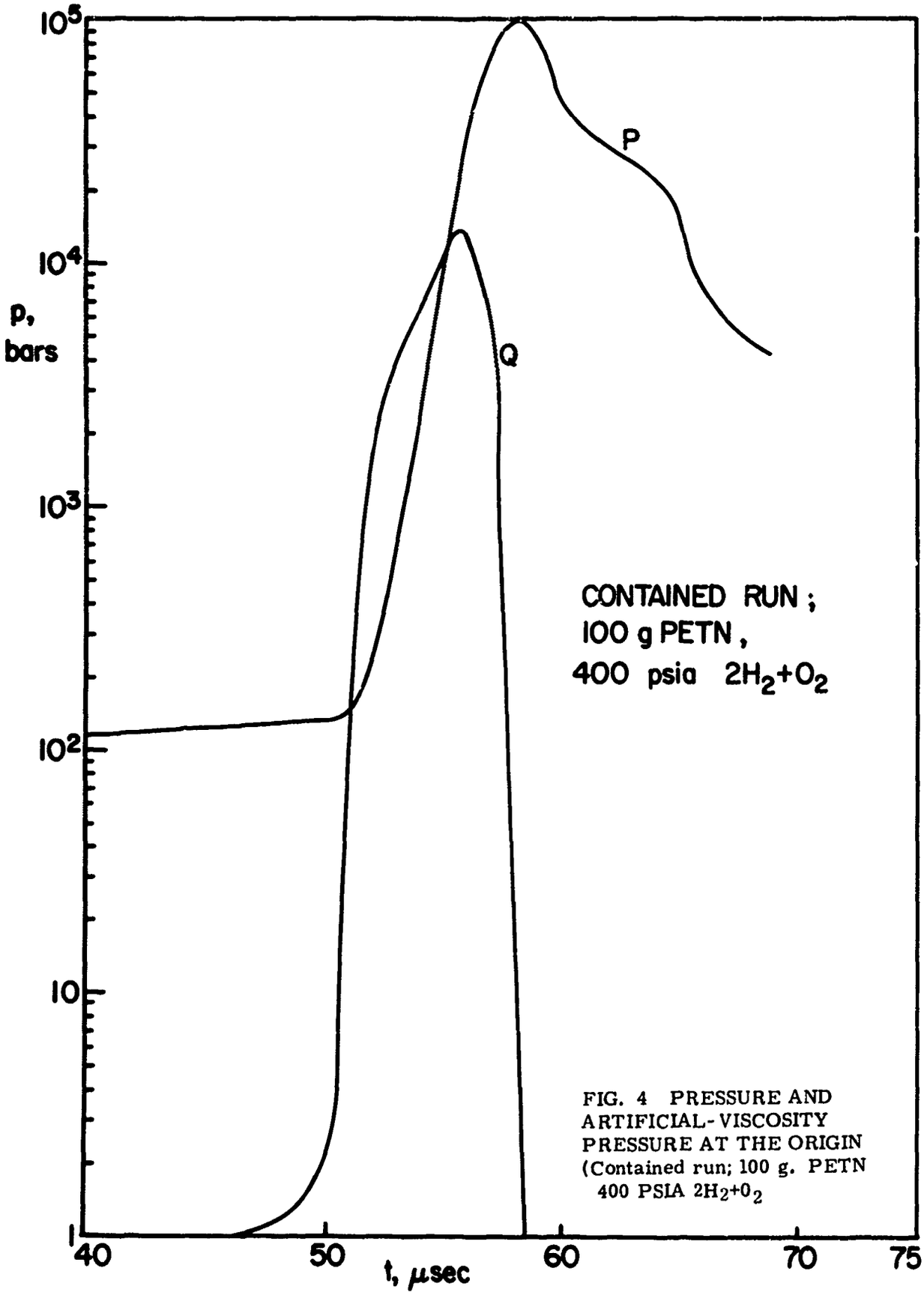

FIG. 4 PRESSURE AND ARTIFICIAL-VISCOSITY PRESSURE AT THE ORIGIN (Contained run; 100 g. PETN 400 PSIA $2H_2+0_2$

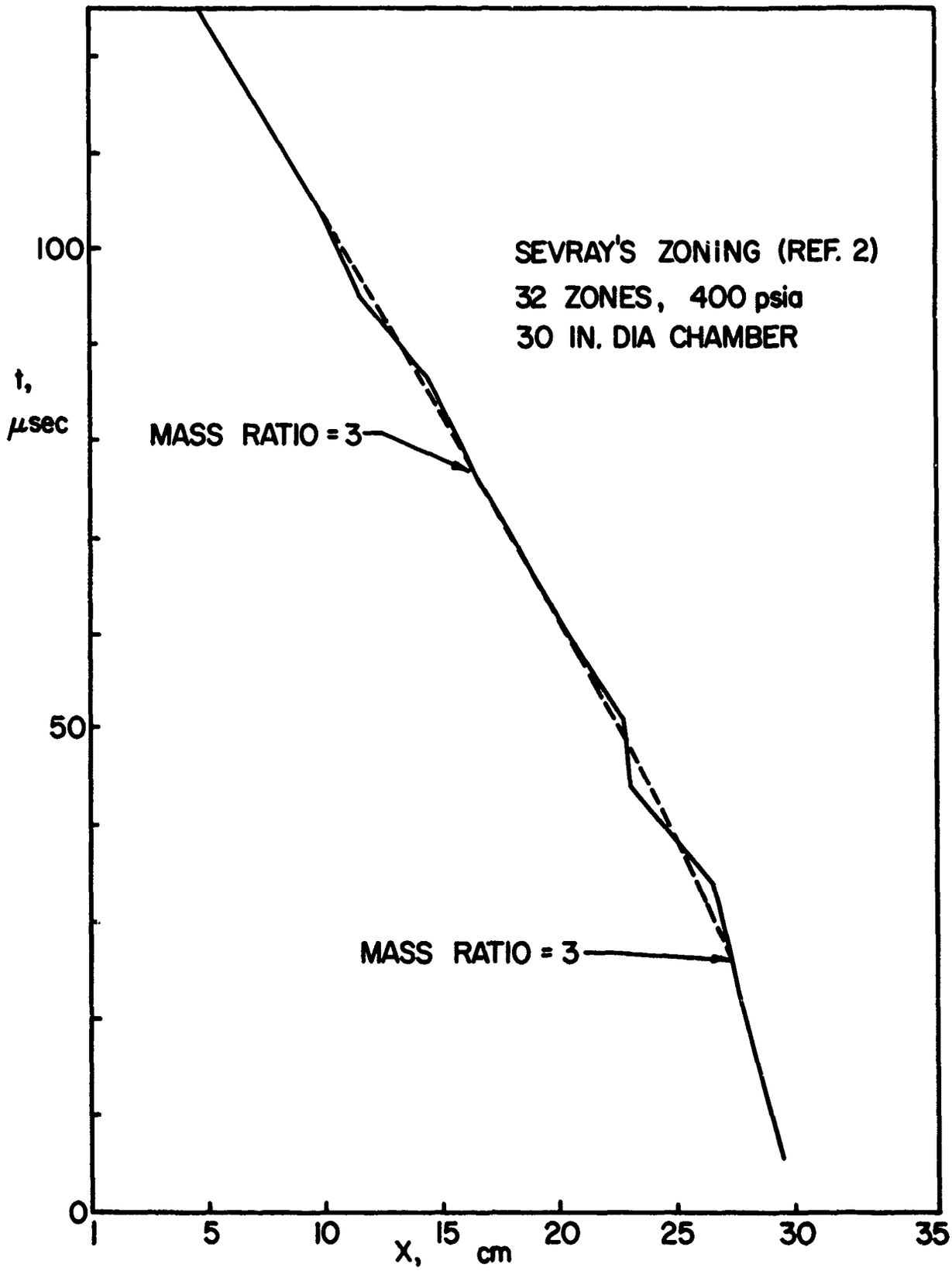

FIG. 5 INFLUENCE OF A CHANGE IN ZONE MASS

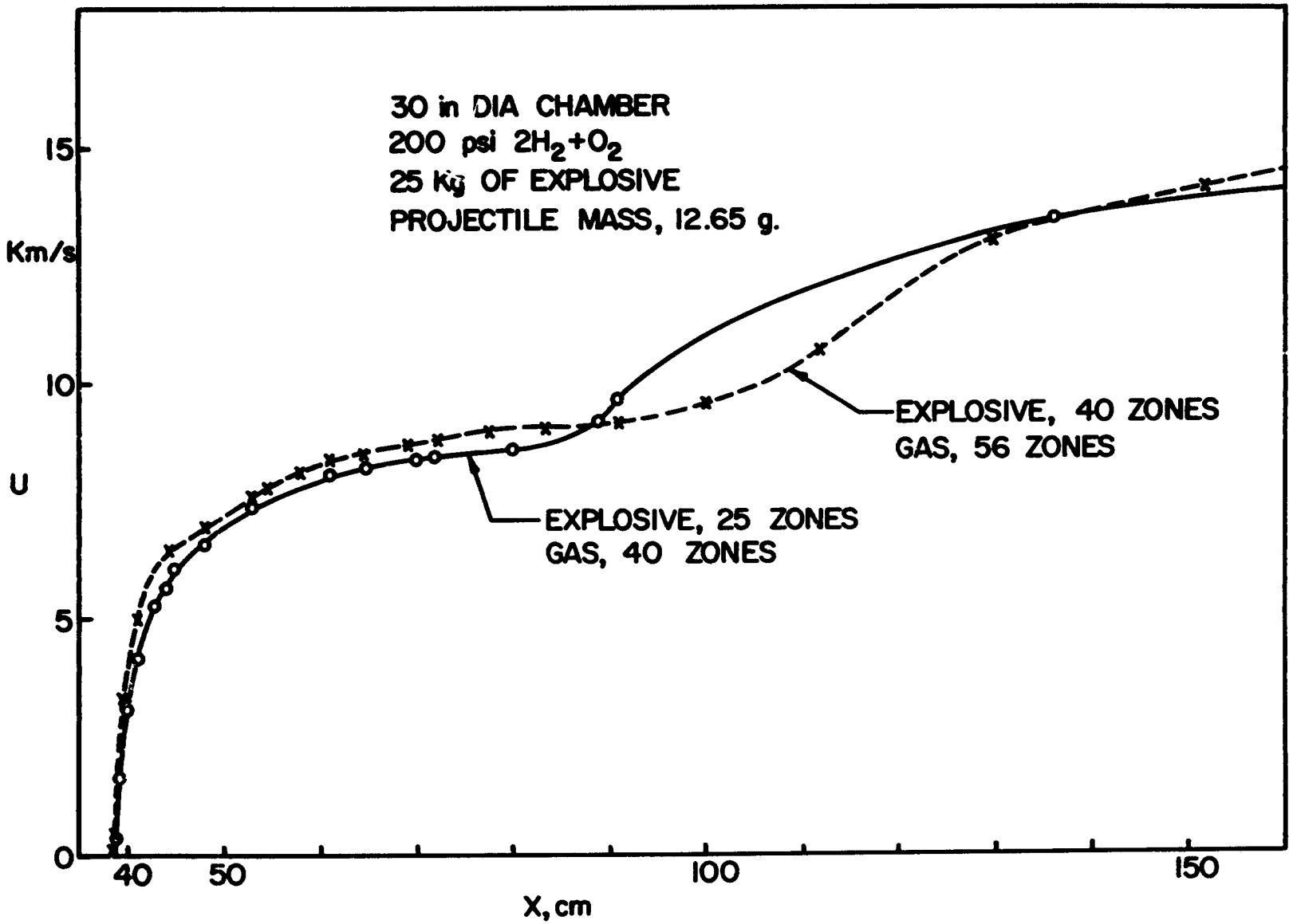

FIG. 6 SEVRAY'S ZONING (REF. 2)
INFLUENCE OF THE NUMBER OF ZONES ON
THE VELOCITY PROFILE

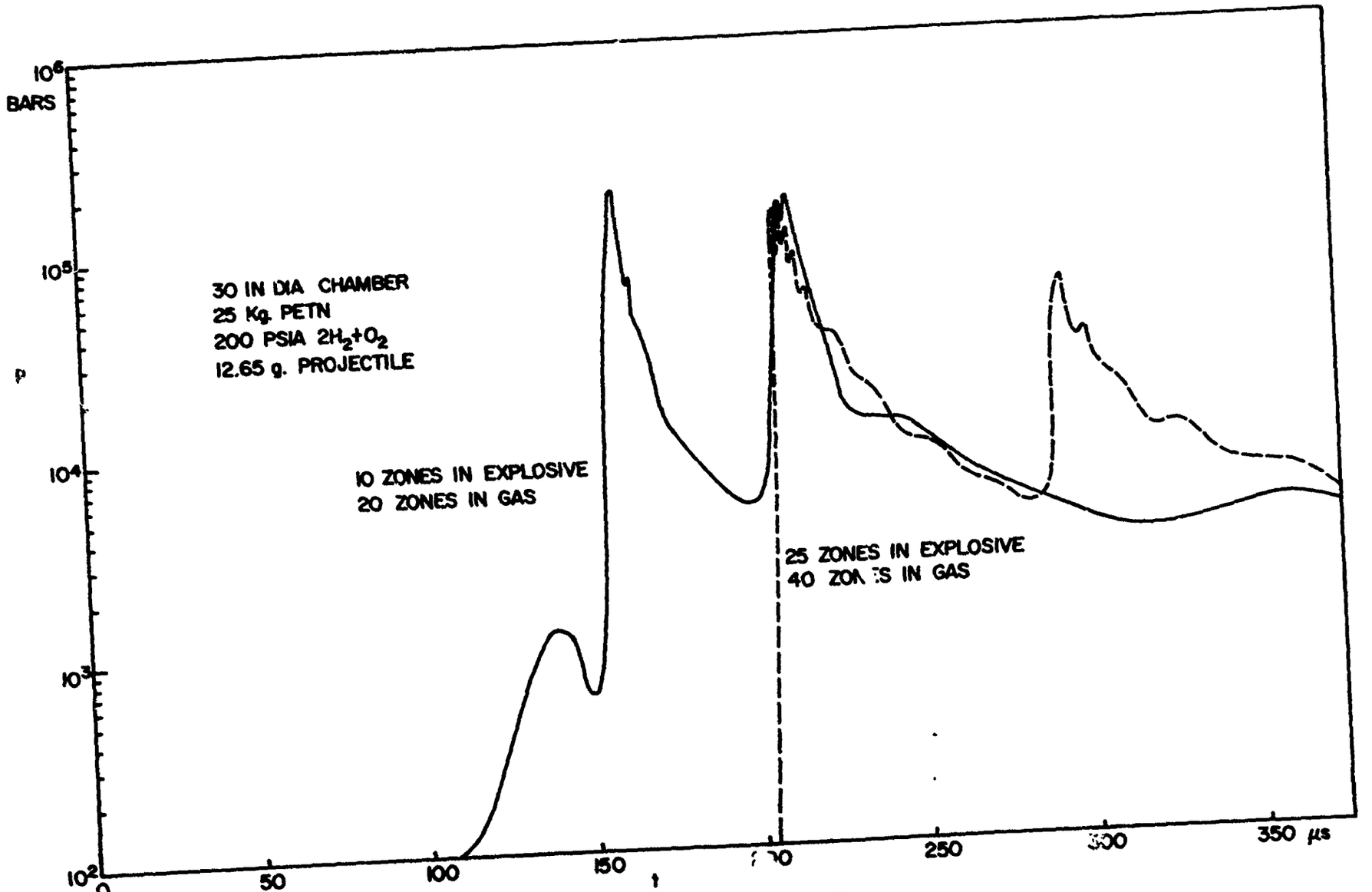

FIG. 7 FLAGG'S ZONING (REF. 3)
INFLUENCE OF THE NUMBER OF ZONES
ON THE PRESSURE ON THE BASE OF THE
PROJECTILE

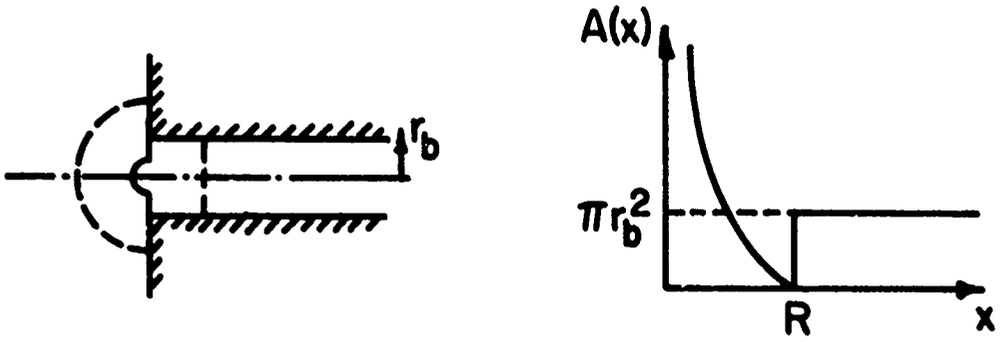

PIACESI'S METHOD (SEE REF. 2)

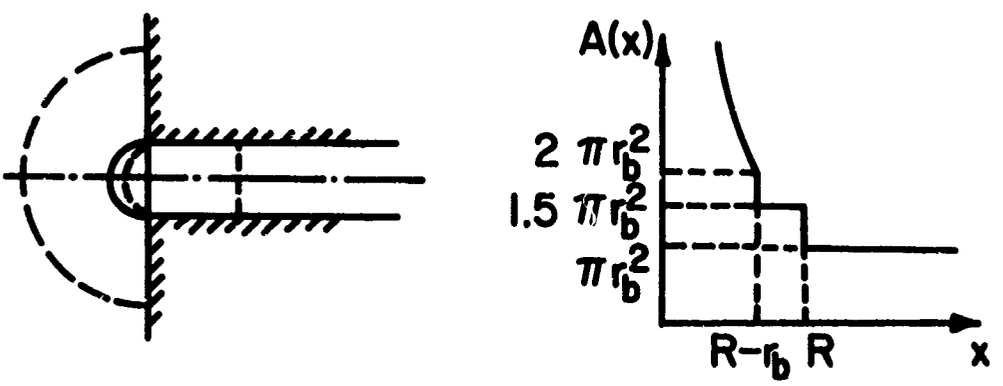

SEVRAY'S METHOD (SEE REF. 2)

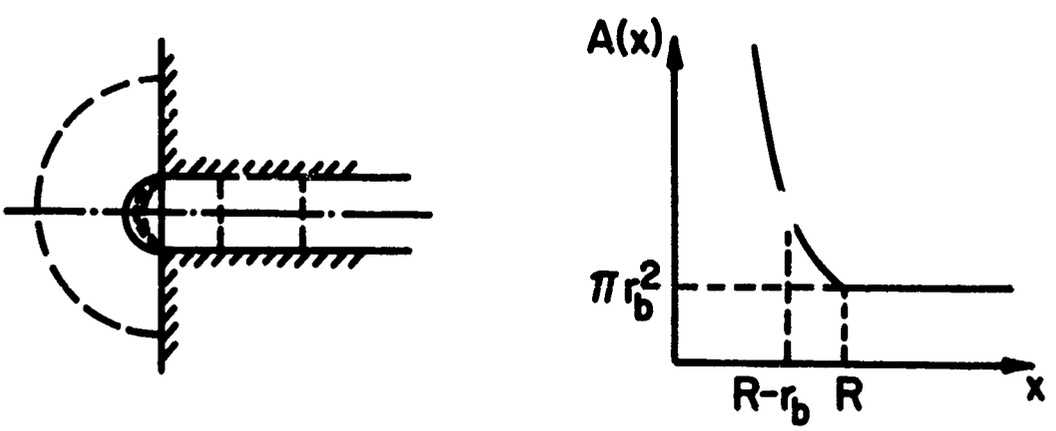

FLAGG'S METHOD (SEE REF. 3)

FIG. 8 TREATMENT OF THE ORIGIN REGION

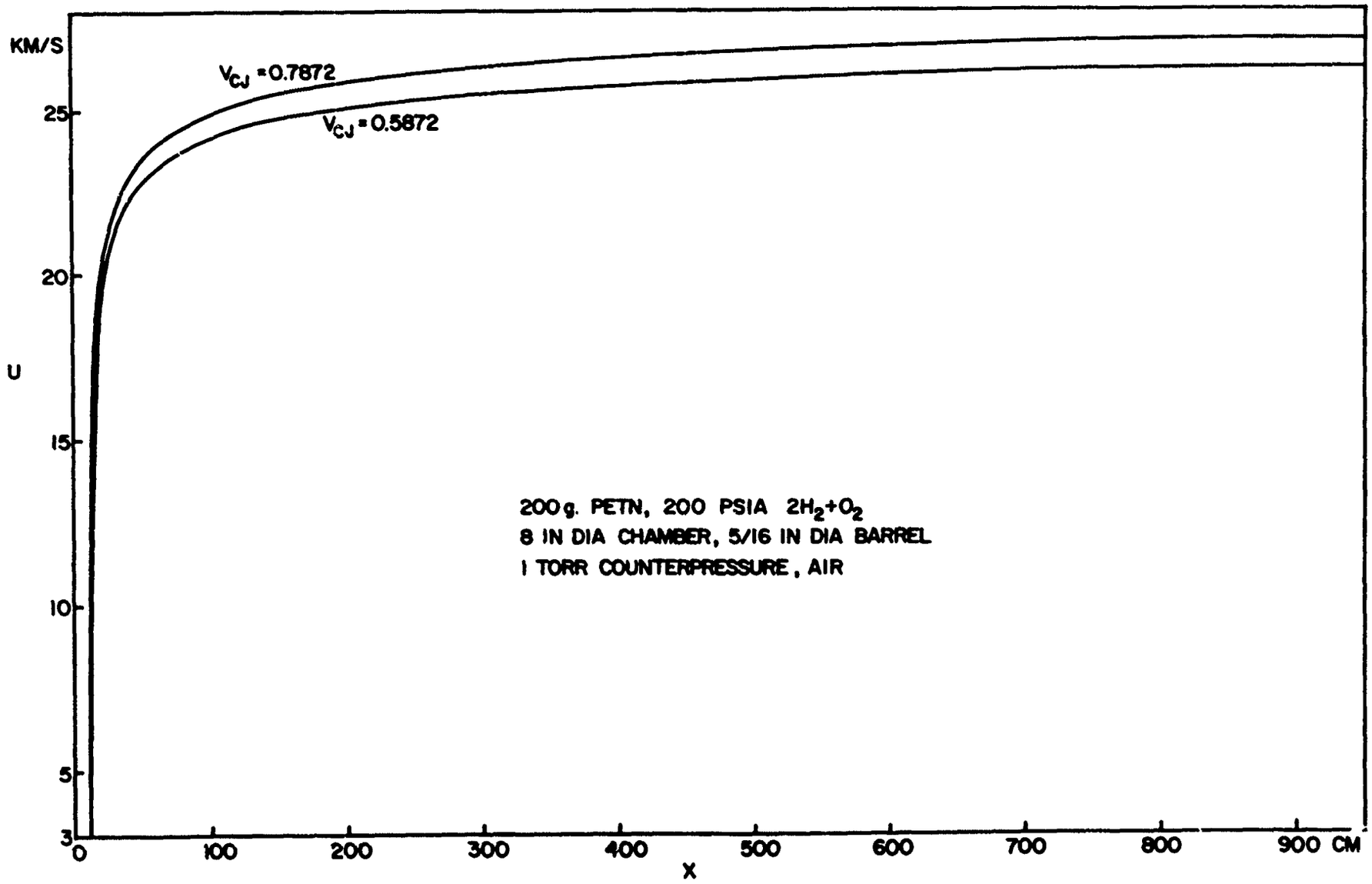

FIG. 9 INFLUENCE OF THE VALUE OF THE CHAPMAN-JOUGUET VOLUME ON THE VELOCITY OF THE INTERFACE

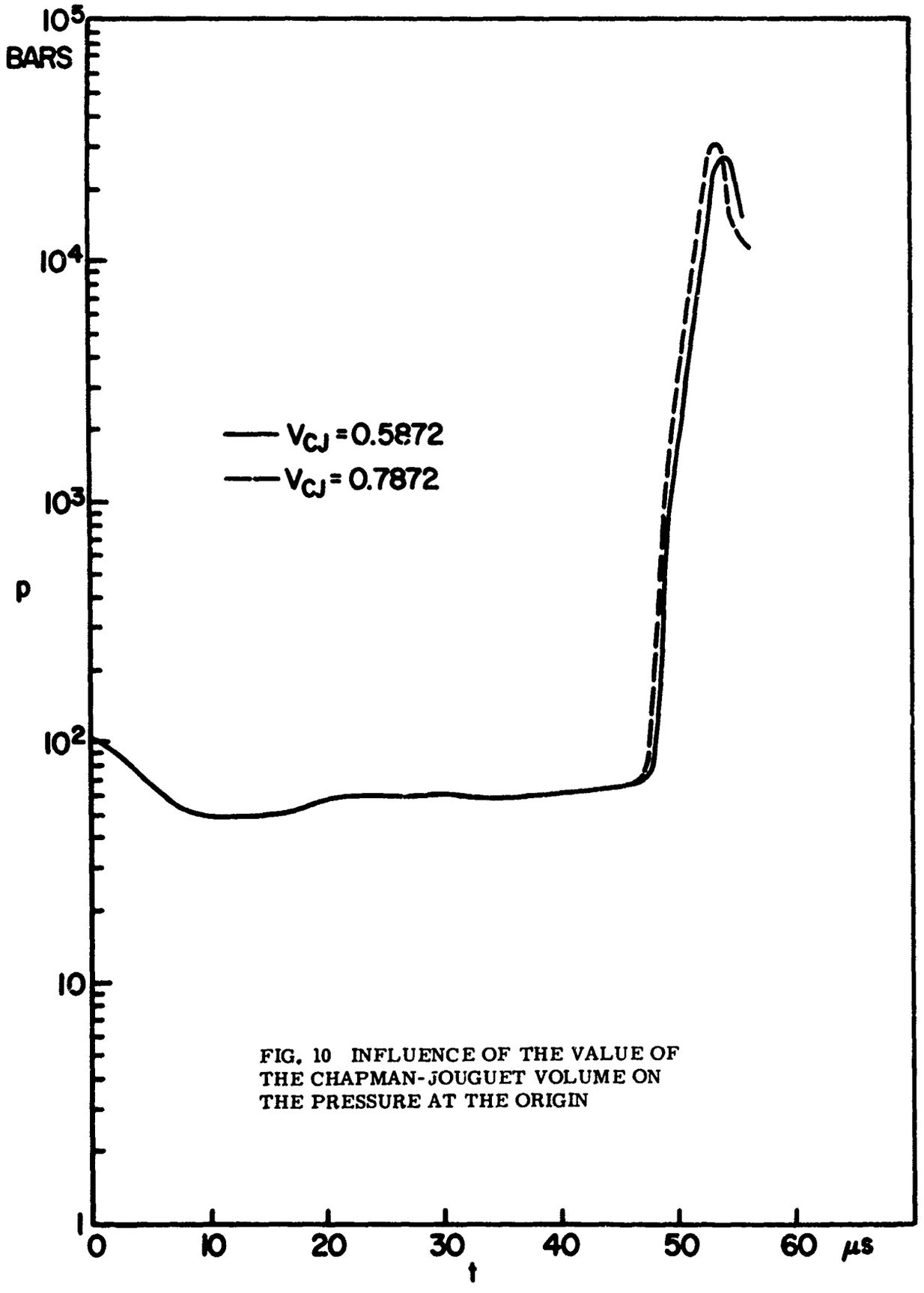

FIG. 10 INFLUENCE OF THE VALUE OF THE CHAPMAN-JOUGUET VOLUME ON THE PRESSURE AT THE ORIGIN

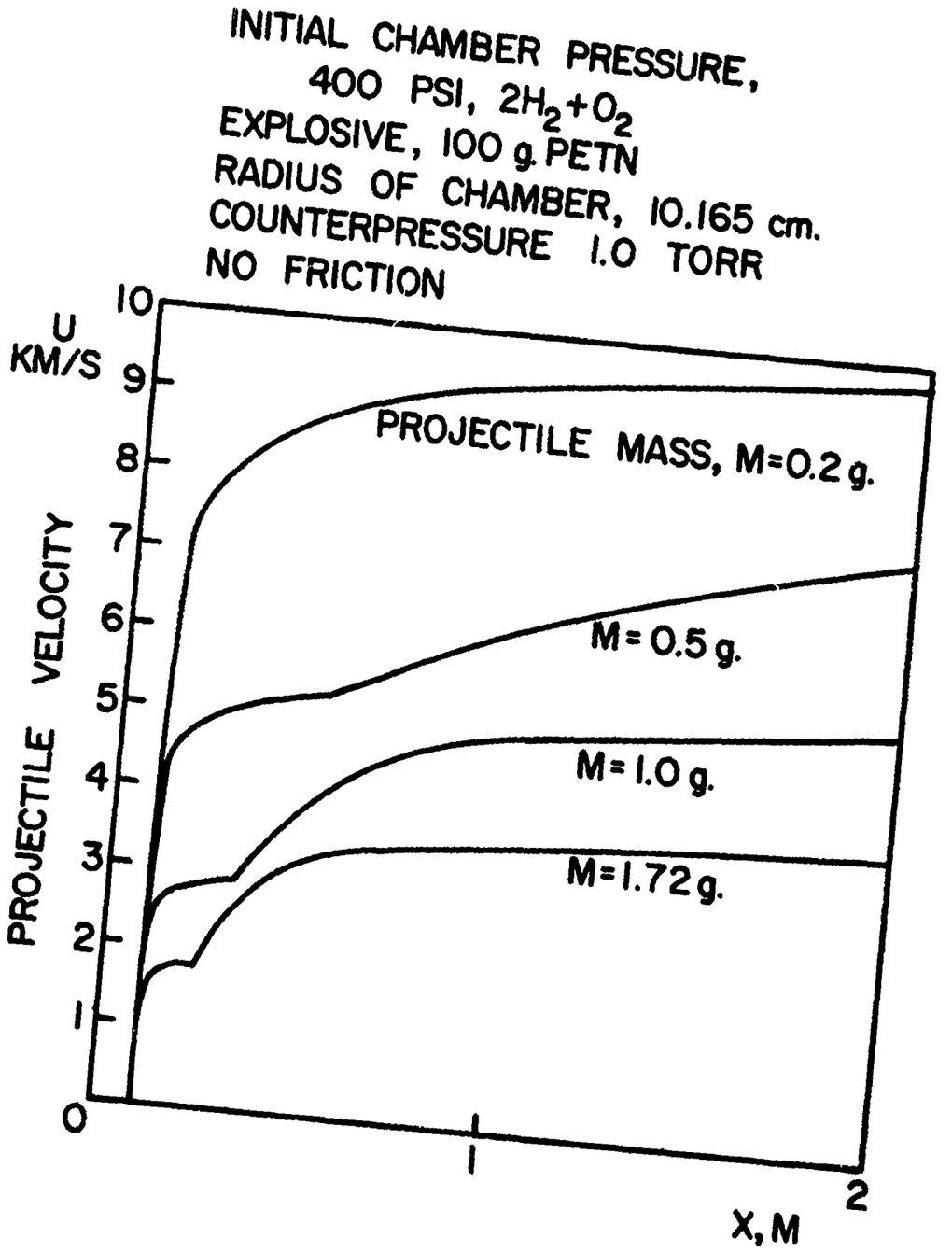

FIG. 11 PROJECTILE VELOCITIES ALONG BARREL FOR VARIOUS PROJECTILE MASSES

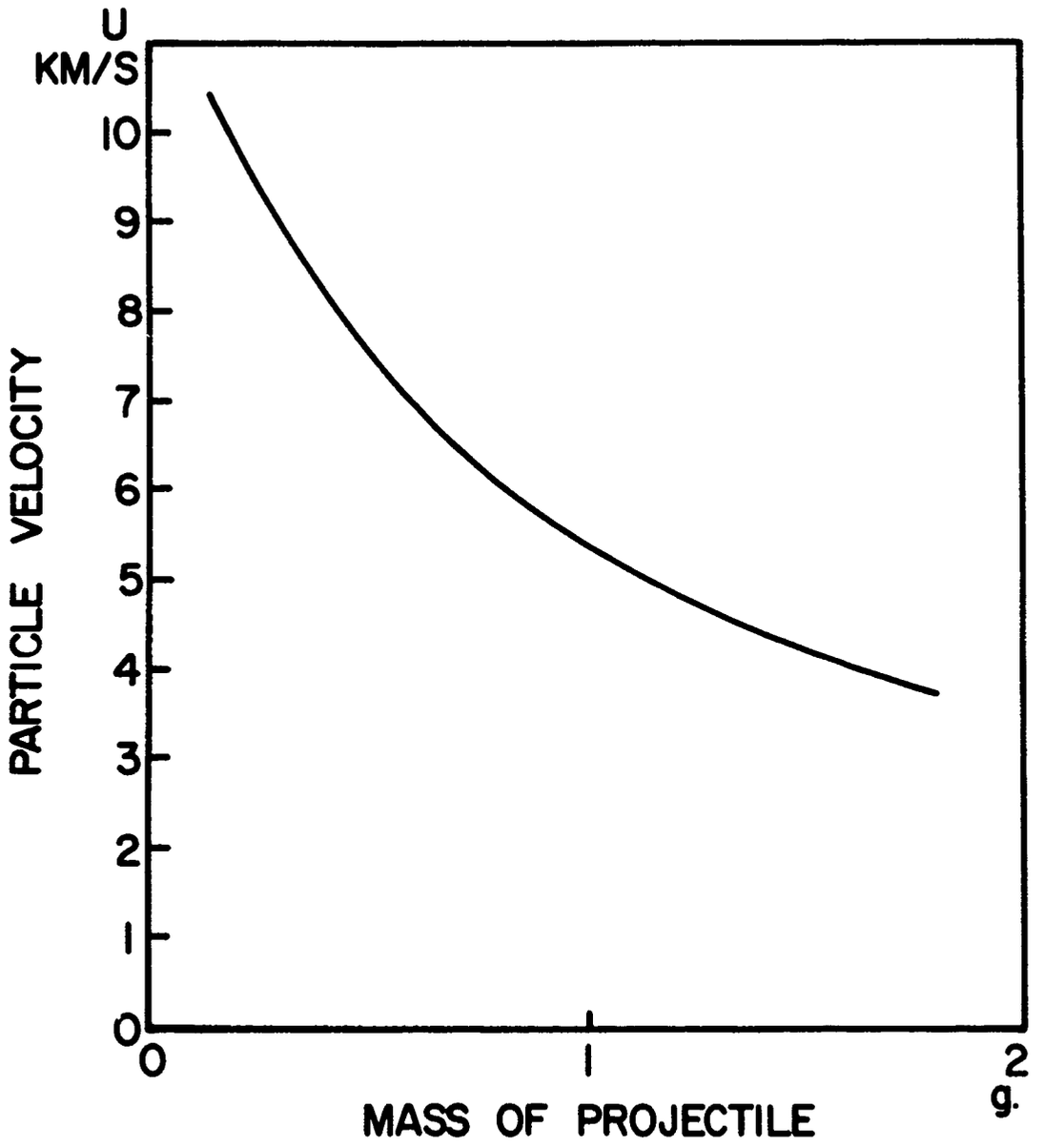

FIG. 12 PROJECTILE VELOCITIES AT TWO METERS DOWNSTREAM OF BARREL AS A FUNCTION OF PROJECTILE MASS
(Computer program failed for Projectile Mass below 0.2 gm.

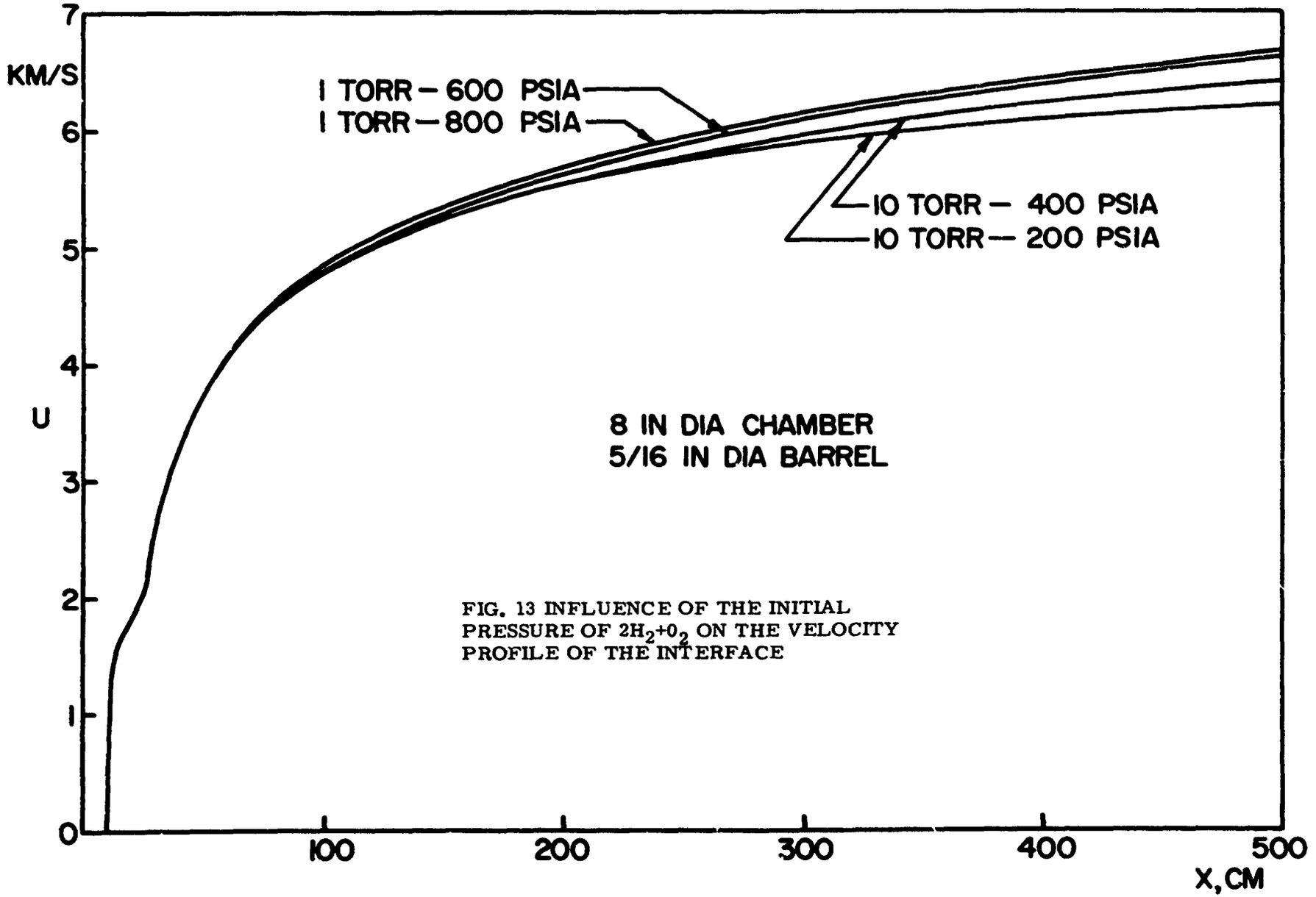

FIG. 13 INFLUENCE OF THE INITIAL PRESSURE OF $2H_2+0_2$ ON THE VELOCITY PROFILE OF THE INTERFACE

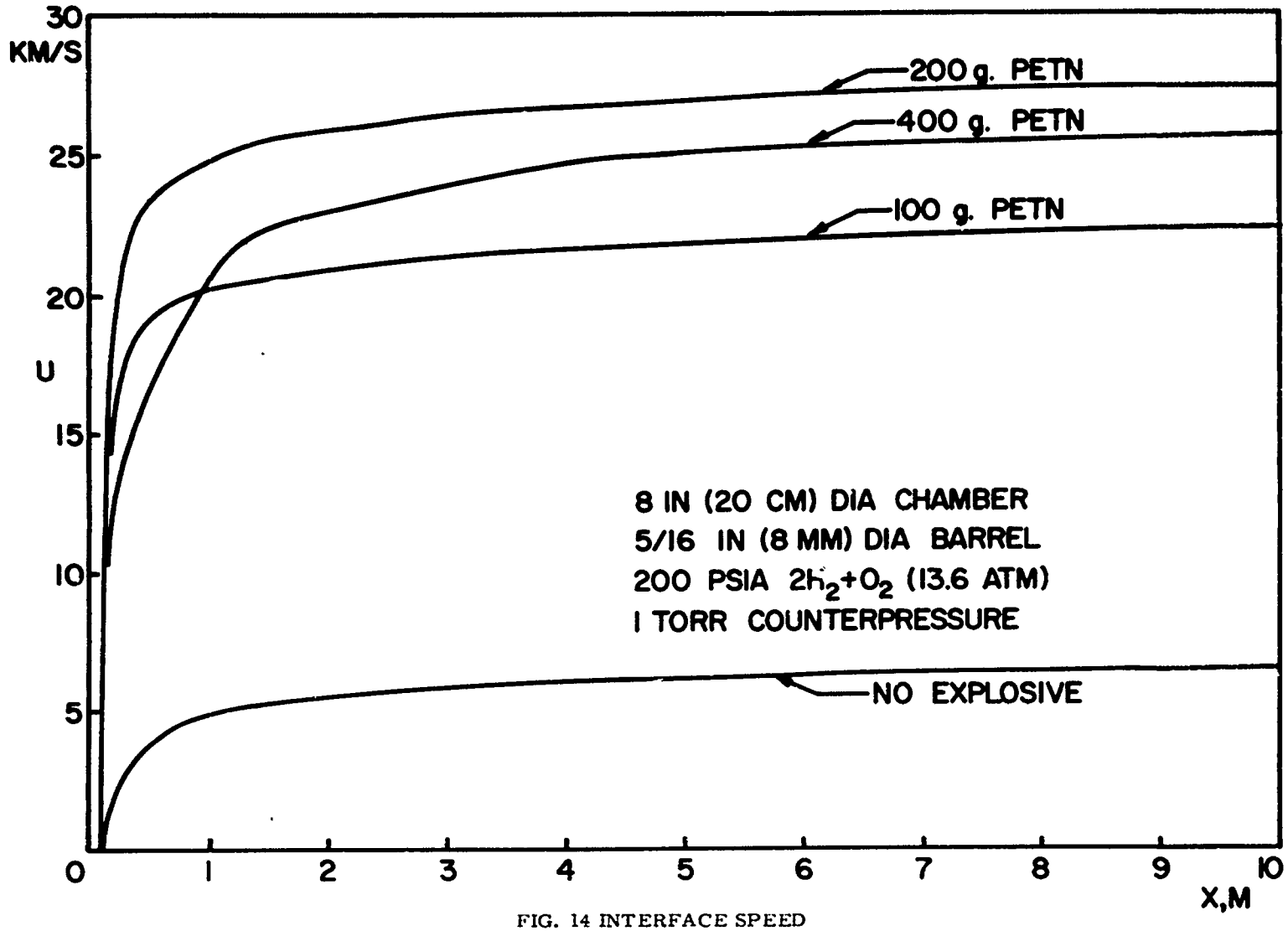

FIG. 14 INTERFACE SPEED
FOR DIFFERENT WEIGHTS
OF EXPLOSIVE

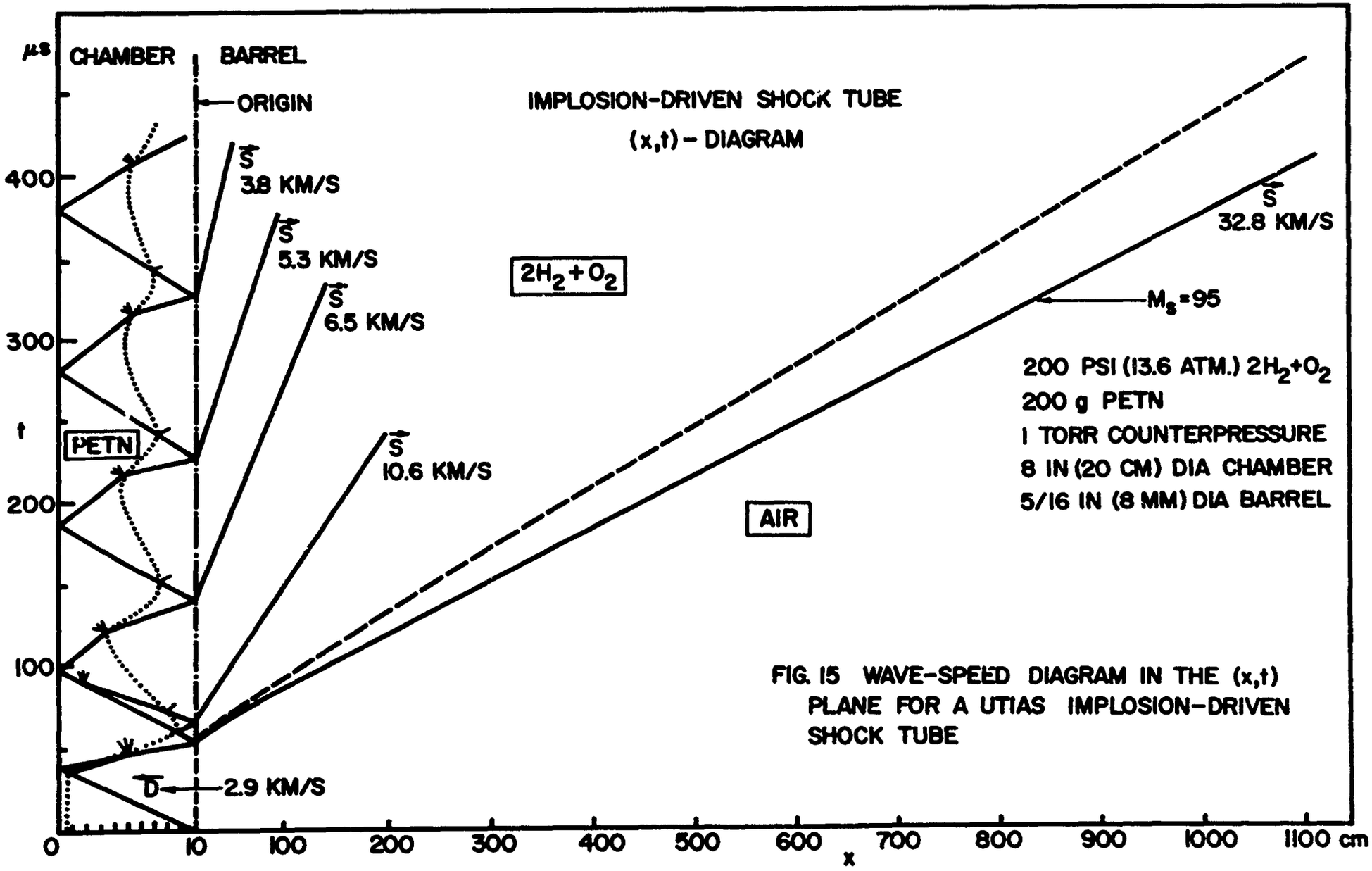

FIG. 15 WAVE-SPEED DIAGRAM IN THE (x,t) PLANE FOR A UTIAS IMPLOSION-DRIVEN SHOCK TUBE

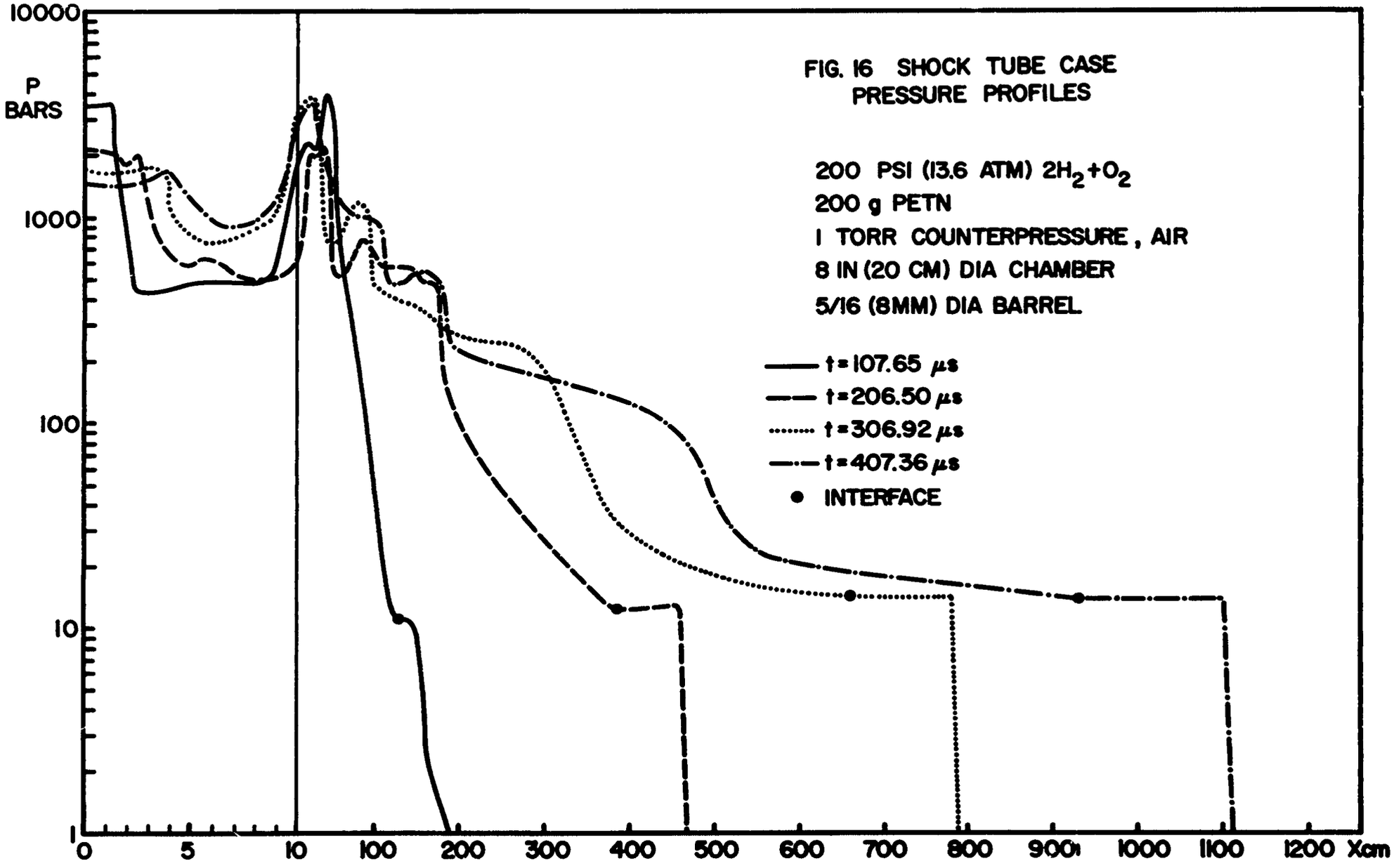
10000
P
BARS
1000
100
10
1
0
5
10
100
200
300
400
500
600
700
800
900
1000
1100
1200
Xcm
FIG. 16 SHOCK TUBE CASE
PRESSURE PROFILES
200 PSI (13.6 ATM) $2H_2+O_2$
200 g PETN
1 TORR COUNTERPRESSURE, AIR
8 IN (20 CM) DIA CHAMBER
5/16 (8MM) DIA BARREL
t=107.65 μs
t=206.50 μs
t=306.92 μs
t=407.36 μs
INTERFACE

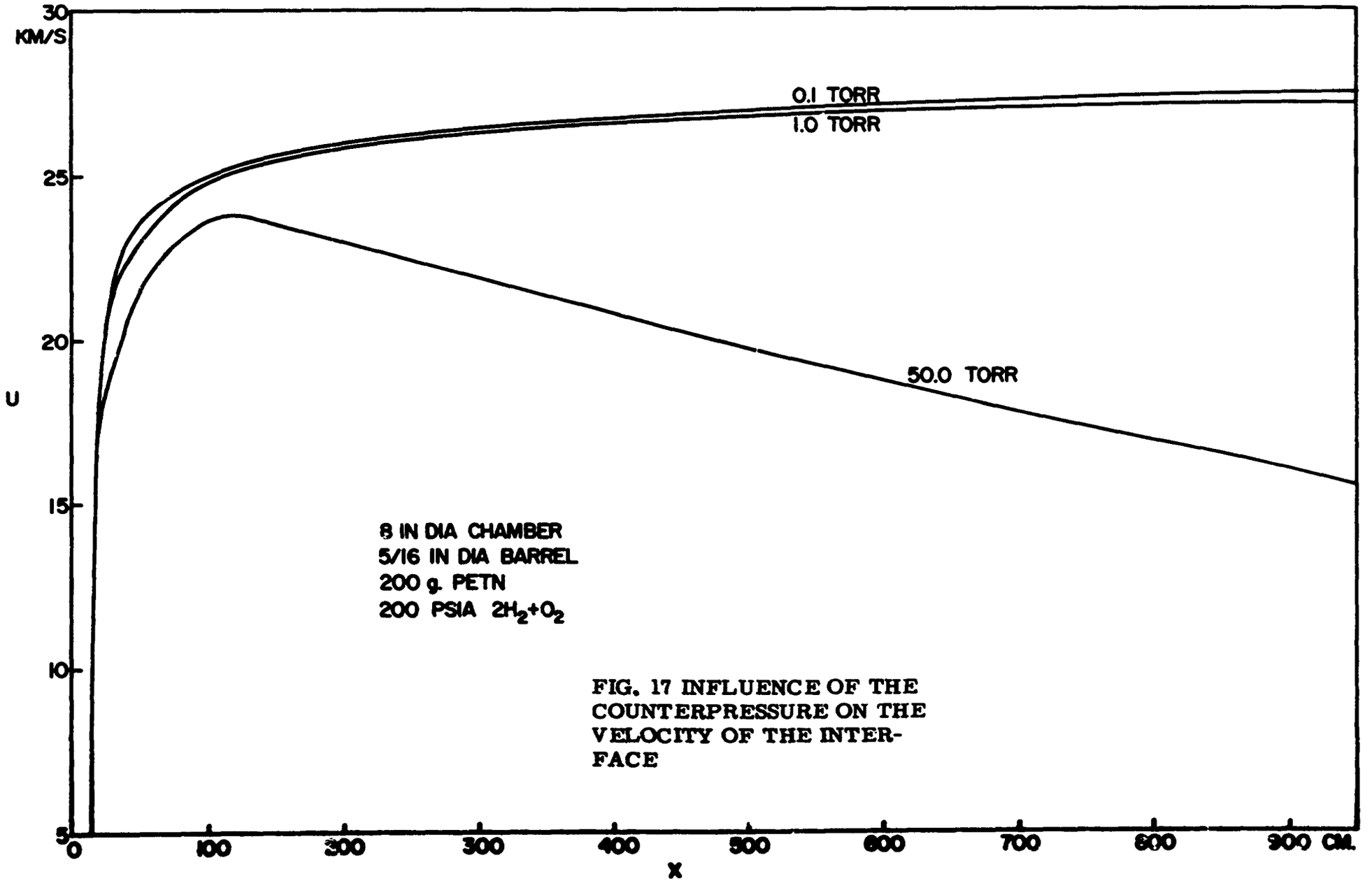

FIG. 17 INFLUENCE OF THE COUNTERPRESSURE ON THE VELOCITY OF THE INTERFACE

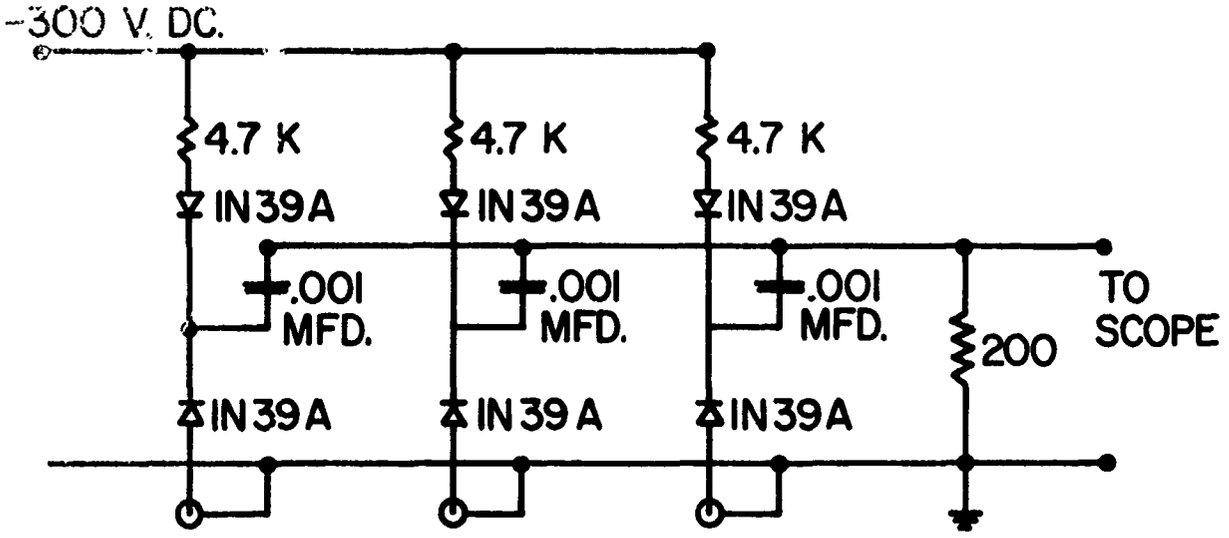

(A) IONIZATION PROBE CIRCUIT USED BY FLAGG (REF. 4) TO DETECT INCIDENT AND REFLECTED WAVES

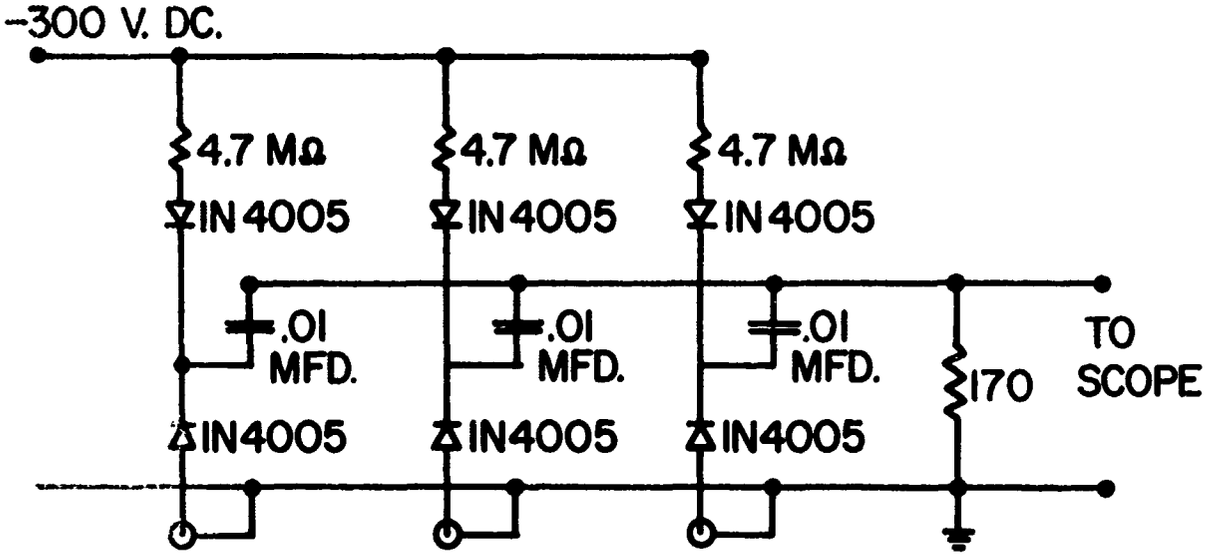

(B) IONIZATION PROBE CIRCUIT ACTUALLY USED

FIG. 18 IONIZATION PROBE CIRCUITS

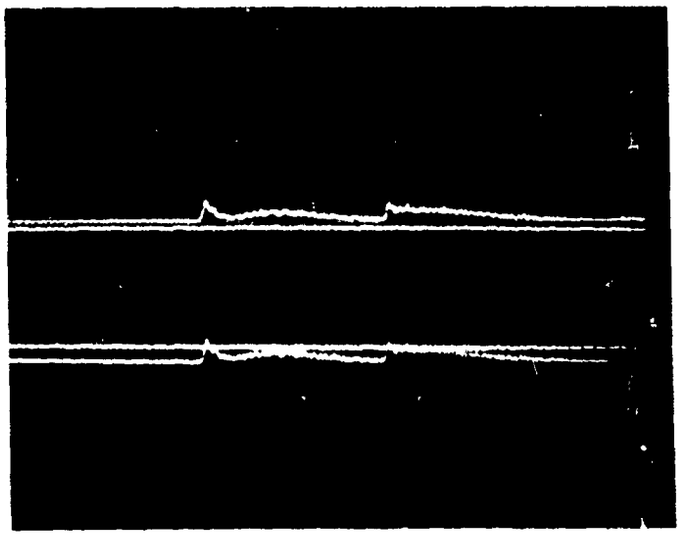

PHOTOMULTIPLIER TRACE

(50 μsec/cm) - The shock arrives at 163 μsec.

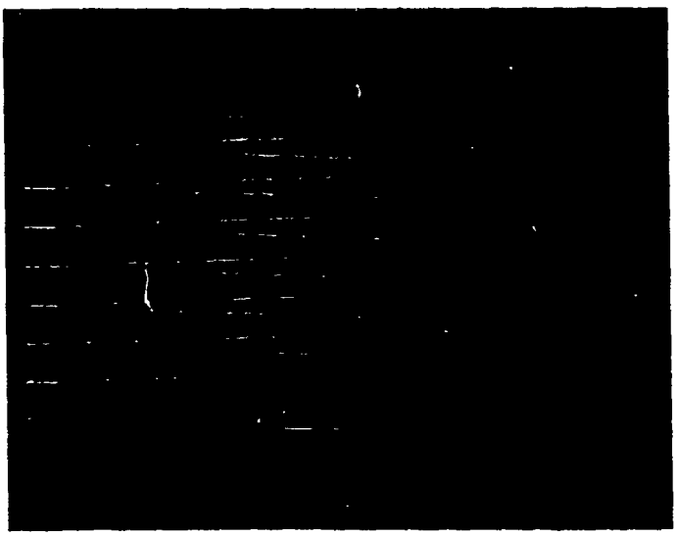

IONIZATION GAUGE TRACE

(10 μsec time marks) - The shock arrives at 167 μsec.

FIG.19: VERIFICATION OF THE IONIZATION GAUGE TECHNIQUE

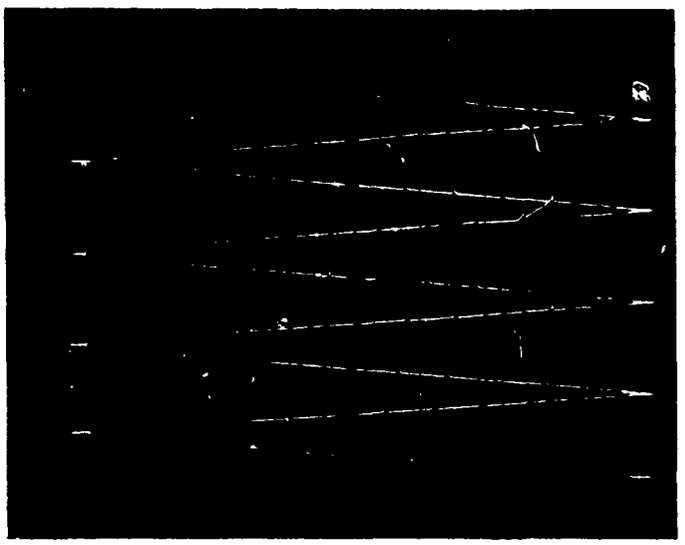

10 μsec time marks delay 76 μsec from ignition

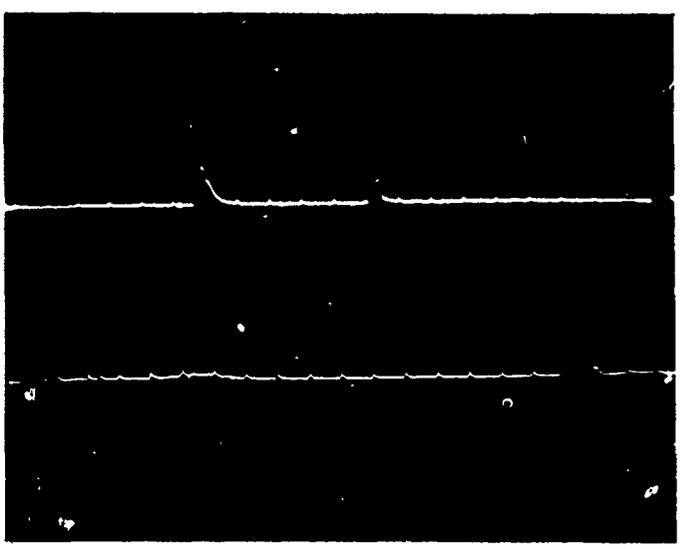

10 μsec time marks

Upper beam delayed 76 μsec - Lower beam delayed 256 μsec.

FIG. 20: IONIZATION GAUGE RECORD

GAS CASE: [illegible] psia dil [illegible]

.05 Torr in the range and channel

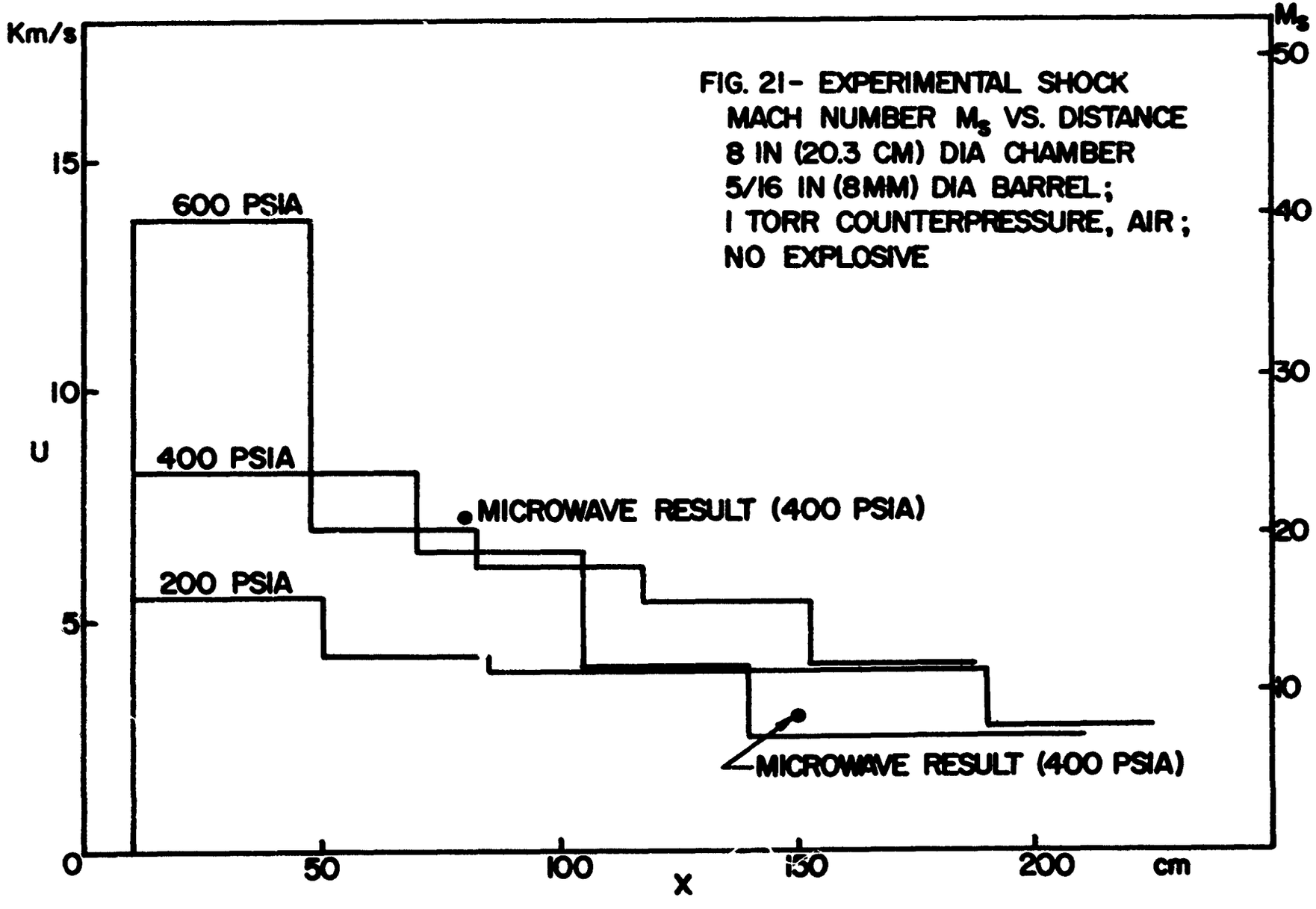

FIG. 21- EXPERIMENTAL SHOCK MACH NUMBER M_s VS. DISTANCE 8 IN (20.3 CM) DIA CHAMBER 5/16 IN (8MM) DIA BARREL; 1 TORR COUNTERPRESSURE, AIR; NO EXPLOSIVE

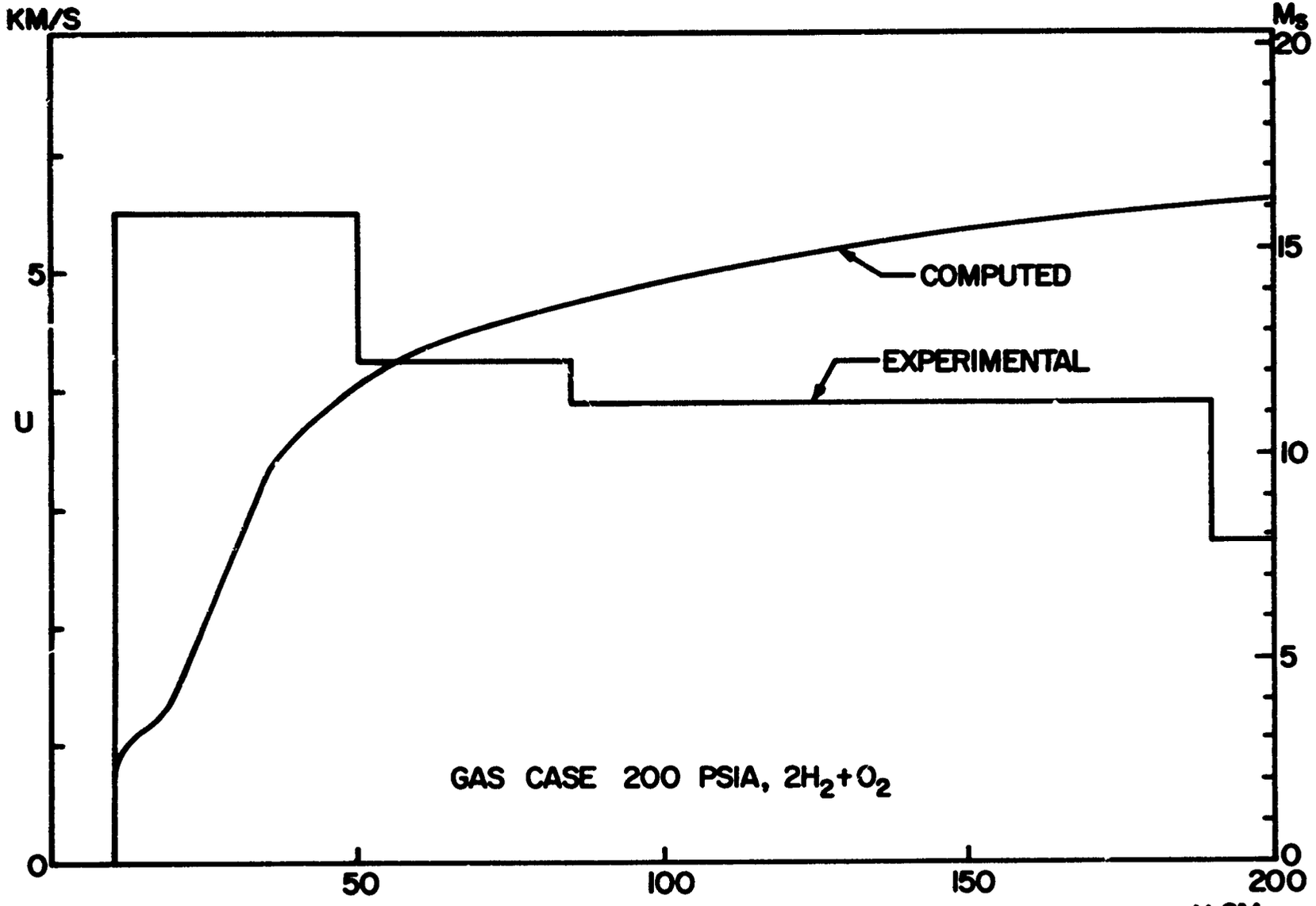

FIG. 22 COMPARISON BETWEEN COMPUTED AND EXPERIMENTAL SHOCK VELOCITIES

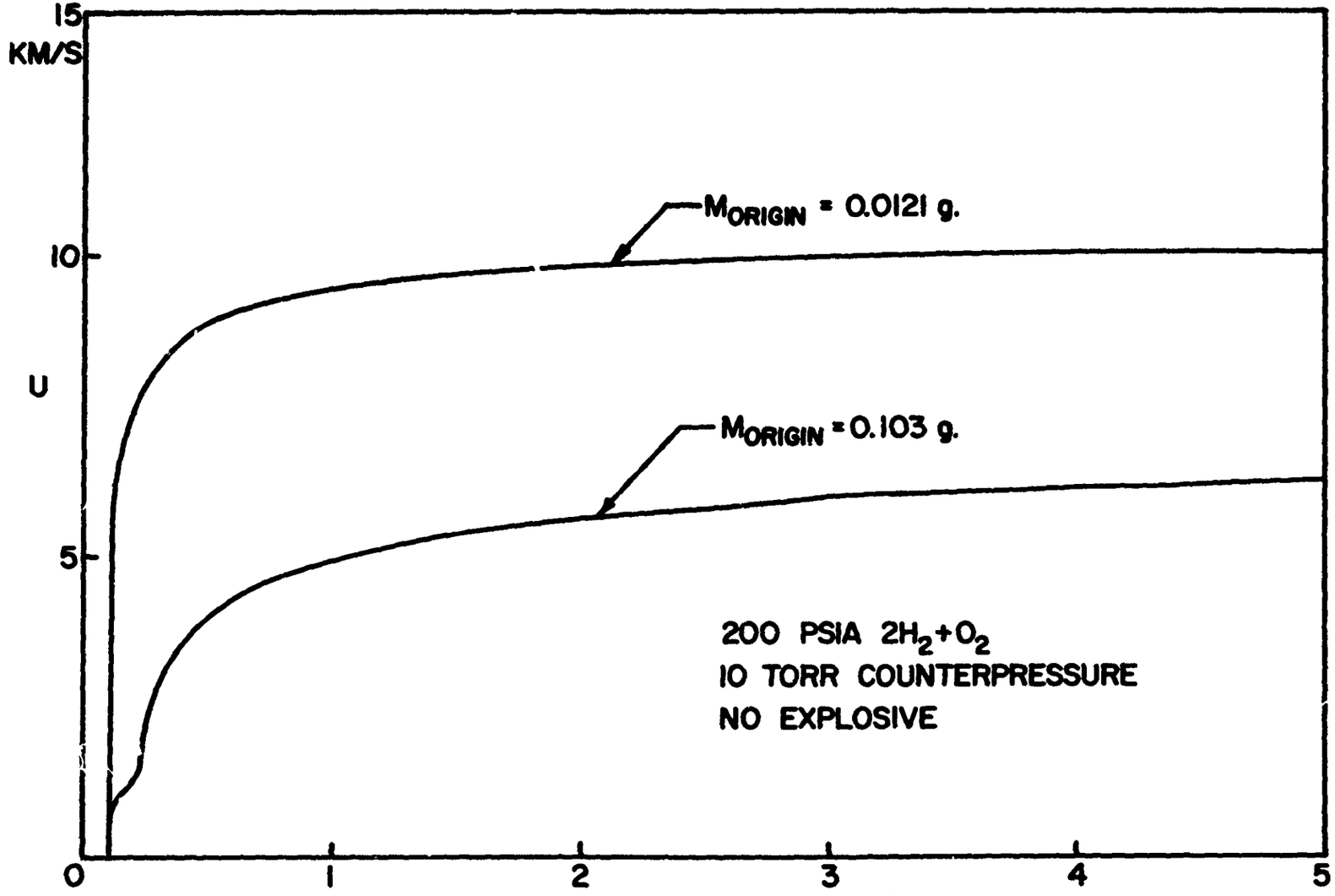

FIG. 23 INFLUENCE OF THE MASS LOCATED AT THE ORIGIN ON THE VELOCITY PROFILE OF THE INTER - FACE

APPENDIX A: SOUND SPEED RELATIONSHIPS

A1: $2H_2+O_2$ mixture

The equation of state is of the form

$$E = E\,(P,V)$$

The speed of sound in a gas is given by the relation

$$c^2 = \left(\frac{\partial p}{\partial \rho}\right)_s = - V^2 \left(\frac{\partial p}{\partial V}\right)_s$$

The total derivative for P is

$$dP = \left(\frac{\partial p}{\partial V}\right)_E dV + \left(\frac{\partial p}{\partial E}\right)_V dE$$

and thus:

$$\left(\frac{\partial p}{\partial V}\right)_s = \left(\frac{\partial p}{\partial V}\right)_E + \left(\frac{\partial p}{\partial E}\right)_V \left(\frac{\partial E}{\partial V}\right)_s$$

The thermodynamic partial derivatives are related by

$$\left(\frac{\partial p}{\partial V}\right)_E \left(\frac{\partial V}{\partial E}\right)_p \left(\frac{\partial E}{\partial p}\right)_v = - 1$$

and

$$\left(\frac{\partial p}{\partial V}\right)_E = \frac{-1}{\left(\frac{\partial E}{\partial p}\right)_V \left(\frac{\partial V}{\partial E}\right)_p}$$

substituting we obtain

$$\left(\frac{\partial p}{\partial V}\right)_s = - p \left(\frac{\partial p}{\partial E}\right)_V - \frac{1}{\left(\frac{\partial E}{\partial p}\right)_V \left(\frac{\partial V}{\partial E}\right)_p}$$

$$= - \left[p \left(\frac{\partial p}{\partial E}\right)_V + \left(\frac{\partial p}{\partial E}\right)_V \left(\frac{\partial E}{\partial V}\right)_p \right]$$

$$= - \left[p + \left(\frac{\partial E}{\partial V}\right)_p \right] \Big/ \left(\frac{\partial E}{\partial p}\right)_V$$

hence:

$$c^2 = v^2 \quad \frac{\left[p + \left(\frac{\partial E}{\partial V}\right)_p \right]}{\left(\frac{\partial E}{\partial p}\right)_V}$$

A2: Explosive

The equation of state is now:

$$P = P(E, V)$$

The relation:

$$\left(\frac{\partial p}{\partial V}\right)_s = \left(\frac{\partial p}{\partial V}\right)_E + \left(\frac{\partial p}{\partial E}\right)_V \left(\frac{\partial E}{\partial V}\right)_s$$

is still valid.

From first low of Thermodynamics

$$dE = TdS - pdV$$

Also,

$$dE = \left(\frac{\partial E}{\partial S}\right)_V dS + \left(\frac{\partial E}{\partial V}\right)_s dV$$

By comparison it becomes:

$$\left(\frac{\partial E}{\partial V}\right)_s = - p$$

and

$$\left(\frac{\partial p}{\partial V}\right)_s = \left(\frac{\partial p}{\partial V}\right)_E - p \left(\frac{\partial p}{\partial E}\right)_s$$

hence,

$$c^2 = v^2 \left[p \left(\frac{\partial p}{\partial E}\right)_V - \left(\frac{\partial p}{\partial V}\right)_E \right]$$

APPENDIX B

PROGRAM LISTING AND FLOW CHARTS

TABLE 1

Summary of Subroutines

DECK NAME	SUBROUTINE NAME	PAGE NUMBER
MAIN		1
READ	LIRE	2
SETUP	DEPOT	3-6
GROS	GUTS	7-8
RETOUR	LFTOV	9-10
OUTPUT	SORT I	11-12
ETAT 1	EQST 1	13-14
ETAT 2	EQST 2	15
ETAT 3	EQST 3	16

APPENDIX B

PROGRAM LISTING AND FLOW CHARTS

```
$IBFTC MAIN     NOLIST
       COMMON AREA1,BRAKE,CSQMA,DLAMA,DTLAS,DUO,EINSU,EKSUM,EMPRO,ESUM,
      1I,IMAX,IQUIT,JLAST,N,N1,N2,NBAR1,NBAR2,NCYCL,NMNHA,NN,NOUTP,
      2NPL3H,NPLHA,NPLUS,PIN3,PINIT,RADIU,SHPR,SIGMA,XBAR1,XSTOP,ZMEXP,
      3T
       COMMON AREA(200,2),BURNE(2),CQSQX(3),CSQ(200),DTMIN(3),DTSQ(200)
      1F(200,2),FINT(3),EKIN(3),F(200,2),HALFM(200),HALFR(3),INTER(4),
      2NZONE(3),P(200,2),PPLUS(200),Q(200,2),ROZER(3),THETA(200),
      3TMINS(2),U(200,2),USQ(200),V(200,2),X(200,2)
     1 CALL LIRE
1100   FORMAT(40X,19H INITIAL CONDITIONS)
1101   FORMAT(35X,15H MASS EXPLOSIVE,9X,F10.2,8H GRAMMES)
1102    FORMAT(35X,17H INITIAL PRESSURE,7X,F10.4,4H PSI)
1103   FORMAT(35X,16H MASS PROJECTILE,8X,F10.4,8H GRAMMES)
1106   FORMAT(35X,22H RADIUS OF THE CHAMBER,2X,F10.4,3H CM)
1107   FORMAT(35X,22H AREA OF THE BARREL   ,2X,F10.4,4H CM2)
1104   FORMAT(1H )
 1108 FORMAT(35X,20HPROJ. RELEASE PRESS.,4X,F10.4,4HBARS)
 1109 FORMAT(35X,15HCOUNTERPRESSURE,9X,F10.4,4HTORR)
       WRITE(6,1104)
       WRITE(6,1104)
       WRITE(6,1100)
       WRITE(6,1104)
       WRITE(6,1101) ZMEXP
       WRITE(6,1104)
       WRITE(6,1102) PINIT
       WRITE(6,1104)
       WRITE(6,1103) EMPRO
       WRITE(6,1104)
       WRITE(6,1106) RADIU
       WRITE(6,1104)
       WRITE(6,1107) AREA1
       WRITE(6,1104)
       WRITE(6,1108) SHPR
       WRITE(6,1104)
       WRITE(6,1109) PIN3
       CALL DEPOT
     2 IF(BRAKE-1.) 803,802,802
   803 IF(PPLUS(JLAST-1)-SHPR) 801,802,802
   801 IMAX=2
       BRAKE=0.
       GO TO 805
   802 IMAX=3
       BRAKE=1.
   805 CALL GUTS
       CALL LFTOV
       IF(IQUIT-1) 2,6,6
     6   IF(DUO) 7,7,1
     7 STOP
       END
```

```
$IBFTC READ     NOLIST
       SUBROUTINE LIRE
       COMMON AREA1,BRAKE,CSQMA,DLAMA,DTLAS,DUO,EINSU,EKSUM,EMPRO,ESUM,
      1I,IMAX,IQUIT,JLAST,N,N1,N2,NBAR1,NBAR2,NCYCL,NMNHA,NN,NOUTP,
      2NPL3H,NPLHA,NPLUS,PIN3,PINIT,RADIU,SHPR,SIGMA,XBAR1,XSTOP,ZMEXP,
      3T
       COMMON AREA(200,2),BURNE(2),CQSQX(3),CSQ(200),DTMIN(3),DTSQ(200),
      1E(200,2),EINT(3),EKIN(3),F(200,2),HALFM(200),HALFR(3),INTER(4),
      2NZONE(3),P(200,2),PPLUS(200),Q(200,2),ROZER(3),THETA(200),
      3TMINS(2),U(200,2),USQ(200),V(200,2),X(200,2)
     1 FORMAT(3I3)
     2 FORMAT(8F10.8)
     3 FORMAT(F10.4)
       READ(5,1) IMAX
       READ(5,2) AREA1,RADIU,XSTOP
       READ(5,3) EMPRO
       READ(5,3) ZMEXP
       READ(5,3) PINIT
       READ(5,2) SHPR
       READ(5,2) PIN3
       READ(5,1) NZONE(1),NZONE(2)
       READ(5,2) XBAR1
       READ(5,1) NBAR1,NBAR2
       READ(5,1) N1,N2
       READ(5,2) DUO
       RETURN
       END
```

```
$IBFTC SETUP   NOLIST
      SUBROUTINE DEPOT
      DIMENSION OUTBD(2),FZERO(3),VZERO(3),DELX(1),GAMMA(3)
      COMMON AREA1,BRAKE,CSQMA,DLAMA,DTLAS,DUO,EINSU,EKSUM,EMPRO,ESUM,
     1I,IMAX,IOUIT,JLAST,N,N1,N2,NBAR1,NBAR2,NCYCL,NMNHA,NN,NOUTP,
     2NPL3H,NPLHA,NPLUS,PIN3,PINIT,RADIU,SHPR,SIGMA,XBAR1,XSTOP,ZMEXP,
     3T
      COMMON AREA(200,2),BURNE(2),CQSQX(3),CSQ(200),DTMIN(3),DTSQ(200),
     1E(200,2),FINT(3),EKIN(3),F(200,2),HALFM(200),HALFR(3),INTER(4),
     2NZONE(3),P(200,2),PPLUS(200),Q(200,2),ROZER(3),THETA(200),
     3TMINS(2),U(200,2),USQ(200),V(200,2),X(200,2)
      BRAKE=0.
      CQSQX(1)=6.
      CQSQX(2)=4.
      CQSQX(3)=4.
      VZERO(1)=1.
      VZERO(2)=1.
      VZERO(3)=1.
      GAMMA(3)=1.4
      BURNE(1)=1.
      BURNE(2)=1.
      OUTBD(2)=RADIU
       ROZER(1)=0.588
      ROZER(2)=12./(14.5*300.*83.70)*PINIT
      ROZER(3)=28.96/(750.0*300.0*83.17)*PIN3
      EZERO(1)=30400.
      EZERO(2)=1.225*1.E 05 *ROZER(2)
      EZERO(3)=PIN3/((GAMMA(3)-1.0)*750.0)
      VEXP=ZMEXP/0.588*3./2./3.1416
      CEXP=RADIU**3-VEXP
      IF(CEXP) 1094,1099,1094
1094  Y1=1.
1095  Y2=Y1-(Y1**3-CEXP)/(3.*Y1**2)
      IF(ABS((Y1-Y2)/Y2) -1.E-4) 1096,1096,1097
1097  Y1=Y2
      GO TO 1095
1096    CURRT=RADIU-Y2
      GO TO 1030
1099   CURRT=0.
1030  OUTBD(1)=CURRT
1000  N=1
1001  NMNHA =N
1002  NPL3H =N
1003  NPLUS =1
1004  NPLHA =NPLUS
1005  NN=3
1006  NOUTP=0
1007  NCYCL =0
1008  T=0.
1009  DTLAS=0.
1010  DTMIN(NN)=0.
1011  INTER (1)=1
1012  DO 35 I=1,IMAX
35    HALFR (I)=ROZER (I)/2.
      NZONE(3)=NBAR1+NBAR2
      DO 40 I=1,IMAX
   40 INTER (I+1)=INTER (I)+NZONE (I)
      JLAST=INTER(IMAX)
```

```
      JLAS3=INTER(IMAX+1)
      JLAS1=JLAST-1
      DNZO1=NZONE(1)
      DELX(1)=                    (RADIU**3-(RADIU-OUTBD(1))**3)/DNZO1
      VGAZ=(RADIU-OUTBD(1))**3
      X(1,N)=0.
       U(1,N)=0.
      DO 55 I=1,IMAX
      IF(I.EQ.1.AND.NZONE(1).EQ.0)  GO TO 55
      JMIN=INTER (I)+1
      JMAX=INTER (I+1)
      DO 51 J=JMIN,JMAX
      JMNHA =J-1
      U(J,NMNHA)=0.
      Q(JMNHA,N)=0.
      V(JMNHA ,N)=VZERO(I)
      E(JMNHA ,N)=EZERO(I)
      U(J,2)=0.
      Q(JMNHA,2)=0.
      V(JMNHA,2)=VZERO(I)
      E(JMNHA,2)=EZERO(I)
      IF(I-2) 101,102,108
C     SETUP       REGION  1  AND  2
 101  DL=J-1
      VOL=DELX(1)*3.14159*0.66666666
      HALFM(JMNHA)=HALFR(I)*VOL
      CJ=RADIU**3-DELX(1)*DL
      GO TO 103
 102  PART=NZONE(2)/2
      M=NZONE(2)/2+NZONE(1)+1
      IF(J-M) 104,104,105
 104  DL=J-1-NZONE(1)
      VOL=4./5.*VGAZ/PART*3.14159*0.6666666
      HALFM(JMNHA)=HALFR(I)*VOL
      CJ=VGAZ-4./5.*VGAZ*DL/PART
      GO TO 103
 105  PART1=NZONE(2)/4
      MP=M+NZONE(2)/4
      IF(J-MP) 106,106,107
 106  DL=J-M
      VOL=3./20.*VGAZ/PART1*3.14159*0.66666666
      HALFM(JMNHA)=HALFR(I)*VOL
      CJ=1.0/5.*VGAZ-3.0/20.0*VGAZ*DL/PART1
      GO TO 103
 107  DL=J-MP
      VOL=1.0/20.0*VGAZ/PART1*3.14159*0.66666666
      HALFM(JMNHA)=HALFR(I)*VOL
      CJ=1.0/20.0*VGAZ*((PART1-DL)/PART1)
 103  IF(CJ) 94,99,94
  94  Y1=1.0
  95   Y2=Y1-(Y1**3-CJ)/(3.*Y1**2)
      IF(ABS((Y1-Y2)/Y2)-1.E-4) 96,96,97
  97  Y1=Y2
      GO TO 95
```

```
 96    CUBRT=Y2
       GO TO 50
 99    CUBRT=0.
       GO TO 50
C      SETUP          REGION  3
  108 P(JMNHA,1)=PIN3/750.
       P(JMNHA,2)=PIN3/750.
       JDJ=J-JLAST
       IF(JDJ-NBAR1) 109,109,110
  109 DELX1=XBAR1/FLOAT(NBAR1)
       VOL=DELX1*AREA1
       HALFM(JMNHA)=VOL*HALER(I)
       DJ=JDJ
       CUBRT=-DJ*DELX1
       GO TO 50
  110 IF(NBAR2) 50,50,111
  111 XBAR2=1.2*XSTOP-(RADIU+XBAR1)
       DELX2=XBAR2/FLOAT(NBAR2)
       VOL=DELX2*AREA1
       HALFM(JMNHA)=VOL*HALFR(I)
       DJ=JDJ-NBAR1
       CUBRT=-XBAR1-DJ*DELX2
C      END       SETUP    REGION  3
 50    X(J,N)=RADIU-CUBRT
   51 X(J,2)=X(J,N)
       U(JMAX+1,NMNHA)=0.
       E(JMAX,N)=EZERO(I)
   55 V(JMAX,N)=VZERO(I)
       JLAS2=JLAS3-1
       HALFM(JLAS3)=HALFM(JLAS2)
       DO 10 J=1,JLAS3
       J=J
       IF(X(J,NPLUS )-RADIU )400,500,500
 400   AREA(J,NPLUS )=((RADIU -X(J,NPLUS ))**2)*2.*3.1416
       GO TO 10
 500   AREA(J,NPLUS )=AREA1
  10   AREA(J,2)=AREA(J,NPLUS)
       P(JLAS3,N)=PIN3/750.
       P(JLAS3,2)=PIN3/750.
       DO 130 I=1,IMAX
       IF(I.EQ.1.AND.NZONE(1).EQ.0)  GO TO 130
       I=I
       IF(I-2) 72,71,73
   72 CALL EQST2
       GO TO 130
   71 JMIN=INTER(I)+1
       JMAX=INTER(I+1)
       JMIN1=JMIN-1
       JMAX1=JMAX-1
       F(JMAX1,N)=0.999
       F(JMAX1,NPLUS)=0.99
       CALL EQST1
       GO TO 130
  73   CALL EQST3
 130   CONTINUE
       DO 135 JMNHA=1,JLAS3
  135 PPLUS (JMNHA )=P(JMNHA ,N)
       EINSU=0.
       EKSUM=0.
```

```
      ESUM=0.
      USQ(1)=U(1,N)**2
      DO 165 I=1,IMAX
      EINT(I)=0.
      EKIN(I)=0.
      IF(I.EQ.1.AND.NZONE(1).EQ.0)  GO TO 165
      JMIN=INTER (I)
      JMAX=INTER (I+1)-1
      DO 160 J=JMIN,JMAX
      JPLHA =J
      USQ(J+1)=U(J+1,N)**2
      EINT(I)=EINT(I)+E(JPLHA ,N)/HALFR (I)*HALFM(JPLHA )
  160 EKIN(I)=(USQ(J)+USQ(J+1))*HALFM(JPLHA )    +EKIN(I)
      EKIN(I)=.5*EKIN(I)
      EINSU =EINSU +EINT(I)
      EKSUM=EKSUM+EKIN(I)
  165 CONTINUE
      ESUM=EINSU +EKSUM
      CALL SORTI
      NPLUS =2
      NPLHA =NPLUS
      DTMIN(NPLHA )=0.00006
      DTMIN(NN)=0.00006
      TMINS (NPLHA )=.00000008
      IQUIT=0
      X(JLAST,NPLUS)=X(JLAST,N)
      RETURN
```

```
$IBFTC GROS     NOLIST
       SUBROUTINE GUTS
       DIMENSION DLAMD(200),TSIGS(200)
       COMMON AREA1,BRAKE,CSQMA,DLAMA,DTLAS,DUO,FINSU,EKSUM,EMPRO,ESUM,
      1I,IMAX,IQUIT,JLAST,N,N1,N2,NBAR1,NBAR2,NCYCL,NYNHA,NN,NOUTP,
      2NPL3H,NPLHA,NPLUS,PINA,PINIT,RADIU,SHPR,SIGMA,XBAR1,XSTOP,ZMEXP,
      3T
       COMMON AREA(200,2),BURNE(2),CQSQX(3),CSQ(200),DTMIN(3),DTSQ(200),
      1E(200,2),EINT(3),EKIN(3),F(200,2),HALFM(200),HALFR(3),INTER(4),
      2NZONE(3),P(200,2),PPLUS(200),Q(200,2),ROZER(3),THETA(200),
      3TMINS(2),U(200,2),USQ(200),V(200,2),X(200,2)
       JLAST=INTER(3)
       JLAS1=JLAST-1
       FRICC=1.0
       DLAMA =0.
       SIGMA =0.
       T=T+DTMIN(NPLHA )
       NCYCL =NCYCL +1
       NOUTP=NOUTP+1
       DO 245 I=1,IMAX
       IF(I.EQ.1.AND.NZONE(1).EQ.0)  GO TO 245
       CSQMA =0.
       X(1,N)=0.
       X(1,NPLUS)=0.
       U(1,NPLHA)=0.
       U(1,NYNHA)=0.
       I=I
       JMIN=INTER (I)+1
       JMAX=INTER (I+1)
       DO 196 J=JMIN,JMAX
       JPLHA =J
       JYNHA =J-1
       IF(JLAST-J) 806,807,806
  807  IF(BRAKE-1.) 808,809,809
  808  DUDT=0.
       GO TO 195
  809  DUDT=FRICC*(PPLUS(JYNHA)-PPLUS(JPLHA))*AREA1/
      1(HALFM(JYNHA)+HALFM(JPLHA)+EMPRO)
       GO TO 195
  806  DUDT=(PPLUS(JYNHA)-PPLUS(JPLHA))*AREA(J,N)/
      1(HALFM(JYNHA)+HALFM(JPLHA))
  195  U(J,NPLHA )=U(J,NYNHA )+DTMIN(NN)*DUDT
  196  X(J,NPLUS )=X(J,N)+DTMIN(NPLHA )*U(J,NPLHA )
       JMIN=INTER(I)+1
       JMAX=INTER(I+1)
C  AREAS  AND  VOLUMES  ARE  NOW  CALCULATED  FOLLOWING  THE  SCHEME
C  OF  FLAGG
       DO 230 J=JMIN,JMAX
       JPLHA=J
       JYNHA=J-1
       PRO=SQRT(AREA1/3.14159)
       IF(X(J,NPLUS)-(RADIU-PRO)) 400,500,500
  400  AREA(J,NPLUS)=(RADIU-X(J,NPLUS))**2*2.0*3.14159
       VOLUM=2.0*3.14159*(RADIU-X(J,NPLUS))**3/3.0
       GO TO 17
  500  IF(X(J,NPLUS)-RADIU) 510,510,520
  510  AREA(J,NPLUS)=3.14159*(RADIU-X(J,NPLUS))**2+AREA1
       IF(X(J-1,NPLUS)-(RADIU-PRO)) 512,512,513
  512  VOLUM=2.0*3.14159*(RADIU-X(J-1,NPLUS))**3/3.0
      1-3.14159*(RADIU-X(J,NPLUS))*((RADIU-X(J,NPLUS))**2+3.0*PRO**2)/6.
       GO TO 17
```

```
513   VOLUM=3.14159*((RADIU-X(J-1,NPLUS))*((RADIU-X(J-1,NPLUS))**2+3.0*
     1PRO**2)-(RADIU-X(J,NPLUS))*((RADIU-X(J,NPLUS))**2+3.0*PRO**2))/6.0
      GO TO 17
520   AREA(J,NPLUS)=AREA1
      IF(X(J-1,NPLUS)-RADIU) 523,522,522
522   VOLUM=AREA1*(X(J,NPLUS)-X(J-1,NPLUS))
      GO TO 17
523   IF(X(J-1,NPLUS)-(RADIU-PRO)) 524,524,525
524   VOLUM=AREA1*(X(J,NPLUS)-RADIU)+2.0*3.14159/3.0*(RADIU-X(J-1,NPLUS)
     1)**3
      GO TO 17
525   VOLUM=AREA1*(X(J,NPLUS)-RADIU)+3.14159/6.0*(RADIU-X(J-1,NPLUS))
     1*((RADIU-X(J-1,NPLUS))**2+3.0*PRO**2)
   17 CONTINUE
      V(JMNHA ,NPLUS )=VOLUM /     HALFM(JMNHA ) *HALFR(I)
      IF(U(J,NPLHA )-U(J-1,NPLHA )) 205,225,225
  205 Q(JMNHA ,NPLHA )=CQSQX (I)    *(U(J,NPLHA )-U(J-1,NPLHA ))
     1**2/(V(JMNHA ,NPLUS )+V(JMNHA ,N)) *HALER(I)
      GO TO 230
  225 Q(JMNHA ,NPLHA )=0.
  230 CONTINUE
      IF(I-2) 83,82,81
   83 CALL EQST2
      GO TO 53
   82 CALL EQST1
      GO TO 53
   81 CALL EQST3
      JMIN=INTER(I)+1
      JMAX=INTER(I+1)
   53 DO 240 J=JMIN,JMAX
      JMNHA =J-1
      TSIGS (JMNHA )=CSQ(JMNHA )/(X(J,NPLUS )-X(J-1,NPLUS ))**2
      PPLUS (JMNHA )=P(JMNHA ,NPLUS )+Q(JMNHA ,NPLHA )
      DLAMD(JMNHA )=CQSQX(I)/2.*(V(JMNHA,N)-V(JMNHA,NPLUS))/
     1(V(JMNHA ,N)+V(JMNHA ,NPLUS ))
      IF(DLAMD(JMNHA)-DLAMA) 600,600,601
  600 DLAMA=DLAMA
      GO TO 620
  601 DLAMA=DLAMD(JMNHA)
  620 IF(TSIGS(JMNHA)-SIGMA)  700,700,701
  700  SIGMA=SIGMA
      GO TO 720
  701 SIGMA=TSIGS(JMNHA)
  720 IF(CSQMA-CSQ(JMNHA)) 800,800,801
  800 CSQMA=CSQ(JMNHA)
      GO TO 240
  801 CSQMA=CSQMA
  240 DTSQ(JMNHA )=.1111111/TSIGS (JMNHA )
  245 CONTINUE
      IF(XSTOP-X(JLAST,NPLUS)) 340,340,246
  340 IQUIT=1
      CALL SORTI
  246 RETURN
      END
```

```
$IBFTC RETOUR  NOLIST
      SUBROUTINE LFTOV
      COMMON AREA1,BRAKE,CSQVA,DLAVA,DTLAS,DUO,EINSU,EKSUM,EMPRO,ESUM,
     1I,IMAX,IQUIT,JLAST,N,N1,N2,NBAR1,NBAR2,NCYCL,NMNHA,NN,NOUTP,
     2NPL3H,NPLHA,NPLUS,PI3,PINIT,RADIU,SHPR,SIGMA,XBAR1,XSTOP,ZMEAN,
     3T
      COMMON AREA(200,2),BURNE(2),CQSQX(3),CSQ(200),DTMIN(3),DISQ(200),
     1E(200,2),EINT(3),EKIN(3),F(200,2),HALFM(200),HALFR(3),INTER(4),
     2NZONE(3),P(200,2),PPLUS(200),Q(200,2),ROZER(3),THETA(200),
     3TMINS(2),U(200,2),USQ(200),V(200,2),X(200,2)
      JLAST=INTER(3)
      DTLAS =DTMIN(NPLHA )
      SIGMI =1./SIGMA
      IF(SIGMI -9.  *TMINS (NPLHA )) 270,270,250
  250 IF(DLAVA -.08 ) 255,270,270
  255 IF(SIGMI -16.  *TMINS (NPLHA )) 265,260,260
  260 IF(DLAVA -.05 ) 270,270,265
  265 TMINS (NPL3H )=TMINS (NPLHA )
      GO TO 285
  270 IF(DLAVA-.005) 275,275,280
  275 TMINS (NPL3H )=SIGMI /4.
      GO TO 285
  280 IF(SIGMI/16. -.005184*TMINS(NPLHA)/DLAVA**2) 400,400,401
  400 TMINS(NPL3H)=SIGMI/16.
      GO TO 285
  401 TMINS(NPL3H)=.005184*TMINS(NPLHA)/DLAVA**2
  285 IF(SQRT(TMINS(NPL3H))-1.4*DTMIN(NPLHA)) 500,500,501
  500 DTMIN(NPL3H)=SQRT(TMINS(NPL3H))
      GO TO 290
  501 DTMIN(NPL3H)=1.4*DTMIN(NPLHA)
  290 DTMIN(NN)=(DTMIN(NPL3H )+DTMIN(NPLHA ))/2.
      NP=NPLUS
      NPLUS =N
      NPLHA =NPLUS
      N=NP
      NMNHA =N
      NPL3H =N
      EINSU =0.
      ESUM=0.
      EKSUM=0.
      USQ(1)=U(1,N)**2
      DO 300 I=1,IMAX
      EINT(I)=0.
      EKIN(I)=0.
      IF(I.EQ.1.AND.NZONE(1).EQ.0)  GO TO 300
      JMIN=INTER (I)
      JMAX=INTER (I+1)-1
      DO 295 J=JMIN,JMAX
      JPLHA =J
      USQ(J+1)=U(J+1,N)**2
      EINT(I)=EINT(I)+E(JPLHA ,N)    *HALFM(JPLHA ) /HALFR(I)
  295 EKIN(I)=(USQ(J)+USQ(J+1))*HALFM(JPLHA )    +EKIN(I)
      EKIN(I)=.5*EKIN(I)
      EINSU =EINSU +EINT(I)
      EKSUM=EKSUM+EKIN(I)
  300 CONTINUE
      EKSUM=EKSUM+.5*EMPRO *U(JLAST,N)**2
      ESUM=EINSU +EKSUM
```

```
      IF(NCYCL-N1) 120,324,324
  324 IF(NOUTP-N2) 120,327,327
  327 NOUTP=0
      CALL SORTI
  120 RETURN
       END
```

```
$IBFTC OUTPUT  NOLIST
      SUBROUTINE SORTI
      DIMENSION ZMASS(200)
      COMMON AREA1,BRAKE,CSQMA,DLAMA,DTLAS,DUO,EINSU,EKSUM,EMPRO,ESUM,
     1T,IMAX,IQUIT,JLAST,N,N1,N2,NBAR1,NBAR2,NCYCL,NMNHA,NN,NOUTR,
     2NPL3H,NPLHA,NPLUS,PIN3,PINIT,RADIU,SHPR,SIGMA,XBAR1,XSTOP,ZMEXP,
     3T
      COMMON AREA(200,2),BURNE(2),CQSQX(3),CSQ(200),DTMIN(3),DTSQ(200),
     1E(200,2),EINT(3),EKIN(3),F(200,2),HALFM(200),HALFR(3),INTER(4),
     2NZONE(3),P(200,2),PPLUS(200),Q(200,2),ROZER(3),THETA(200),
     3TMINS(2),U(200,2),USQ(200),V(200,2),X(200,2)
      IMAX=3
      JLAST=INTER(IMAX)
      JLAS1=JLAST-1
      JLAS3=INTER(IMAX+1)
      JLAS2=JLAS3-1
  421 FORMAT(1HO)
    1 FORMAT(1H1)
    2 FORMAT(3X,115HJ     X(J,N)       U(J,N-1/2)    V(J+1/2,N)    P(J+1/2,N
     1) Q(J+1/2,N-1/2) E(J+1/2,N)  AREA(J,N) DTSQ(1/2,1/2)  DM(J+1/2))
    3 FORMAT(3X,111H       CM           CM/MILLISEC   CC/CCO          BARS
     1       BARS       BARS-CC/G                   MILLISECSQ   GRAMS)
    4 FORMAT(I4,  6E13.5,2E11.3,E13.5)
    6 FORMAT(I5,  3E15.5)
    7 FORMAT(3X,116HJ     X(J,N)       U(J,N-1/2)    V(J+1/2,N)    P(J+1/2,N
     1) Q(J+1/2,N-1/2) E(J+1/2,N) AREA(J,N)  DTSQ(1/2,1/2)   TEMPR    )
    8 FORMAT(3X,111H       CM           CM/MILLISEC   CC/CCO          BARS
     1       BARS       BARS-CC/G                   MILLISECSQ    DEGK)
   12 FORMAT(47H CYCLE       T                DT              TOTAL E)
      ILIMI  =IMAX
      WRITE(6,1)
      WRITE(6,12)
      WRITE(6,6) NCYCL ,T,DTLAS ,ESUM
      WRITE(6,421)
      IF(NCYCL) 53,53,64
   53 DO 57 JPLHA=1,JLAS2
   57 ZMASS(JPLHA)=2.*HALFM(JPLHA)
      WRITE(6,2)
      WRITE(6,3)
      WRITE(6,421)
      DO 604 L=1,JLAS2
      IF(L-INTER(3)) 601,603,602
  601 IF(L-INTER(2)) 602,603,602
  602 WRITE(6,4) L,X(L,N),U(L,NMNHA),V(L,N),PPLUS(L),Q(L,NMNHA),
     1E(L,N),AREA(L,N),DTSQ(L),ZMASS(L)
      GO TO 604
  603 IF(L.EQ.INTER(2).AND.NZONE(1).EQ.0)  GO TO 602
      WRITE(6,421)
      WRITE(6,4) L,X(L,N),U(L,NMNHA ),V(L,N),PPLUS (L),Q(L,NMNHA ),
     1E(L,N),AREA(L,N),DTSQ(L),ZMASS(L)
  604 CONTINUE
   41 FORMAT(I4,  2E13.5,74X,E13.5)
      WRITE(6,41) JLAST,X(JLAST,N),U(JLAST,NMNHA),EMPRO
      GO TO 71
   64 IF(BRAKE-1.) 80,81,81
   80 L2=JLAS1
      GO TO 65
```

```
   81 JL1=JLAST+1
      DO 82 J=JL1,JLAS3
      JMNHA=J-1
      APIN=2.*PIN3/750.
      IF(PPLUS(JMNHA)-APIN) 83,83,82
   83 L2=J
      GO TO 65
   82 CONTINUE
   65 WRITE(6,7)
      WRITE(6,8)
      WRITE(6,421)
      DO 704 L=1,L2
      ILIMI=IMAX
      DO 702 IL=2,ILIMI
      IF(L-INTER(IL)) 702,703,702
  702 CONTINUE
  705 WRITE(6,4) L,X(L,N),U(L,NMNHA),V(L,N),PPLUS(L),Q(L,NMNHA),
     1E(L,N),AREA(L,N),DTSQ(L),THETA(L)
      GO TO 704
  703 IF(IL.EQ.2.AND.NZONE(1).EG.0)  GO TO 705
      WRITE(6,421)
      WRITE(6,4) L,X(L,N),U(L,NMNHA),V(L,N),PPLUS(L),Q(L,NMNHA),
     1E(L,N),AREA(L,N),DTSQ(L),THETA(L)
  704 CONTINUE
      WRITE(6,4) JLAST,X(JLAST,N),U(JLAST,NMNHA)
   71 CONTINUE
      RETURN
      END
```

```
$IBFTC ETAT1   NOLIST
       SUBROUTINE EQST1
       COMMON AREA1,BRAKE,CSQMA,DLAMA,DTLAS,DUO,EINSU,EKSUM,EMPRO,ESUM,
      1I,IMAX,IOUIT,JLAST,N,N1,N2,NBAR1,NBAR2,NCYCL,NMNHA,NN,NOUTP,
      2NPL3H,NPLHA,NPLUS,PIN3,PINIT,RADIU,SHPR,SIGMA,XBAR1,XSTOP,ZMEXP,
      3T
       COMMON AREA(200,2),BURNE(2),CQSQX(3),CSQ(200),DTMIN(3),DTSQ(200),
      1E(200,2),EINT(3),EKIN(3),F(200,2),HALFM(200),HALFR(3),INTER(4),
      2NZONE(3),P(200,2),PPLUS(200),Q(200,2),ROZER(3),THETA(200),
      3TMINS(2),U(200,2),USQ(200),V(200,2),X(200,2)
       I=2
       JMIN=INTER(I)+1
       JMAX=INTER(I+1)
       JMIN1=JMIN-1
       JMAX1=JMAX-1
       IF(BURNE (I)) 1,10,1
     1 FMIN=2.
       IF(NCYCL) 500,500,501
   500 JMAX2=JMAX1-1
       GO TO 502
   501 JMAX2=JMAX1
   502 DO 66 JMNHA=JMIN1,JMAX2
       F(JMNHA ,NPLUS )=(1.-V(JMNHA ,NPLUS ))/(1.-.54)
       IF(F(JMNHA,NPLUS)-.001)2,3,3
     2 F(JMNHA ,NPLUS )=0.
     3 IF(F(JMNHA ,NPLUS )-1.) 4,6,5
     4 IF(F(JMNHA ,NPLUS )-F(JMNHA ,N)) 5,6,6
     5 F(JMNHA ,NPLUS )=1.
     6 IF(F(JMNHA,NPLUS)-FMIN) 300,300,301
   300 FMIN=F(JMNHA,NPLUS)
       GO TO 66
   301 FMIN=FMIN
    66 CONTINUE
       IF(FMIN-1.) 10,7,7
     7 DO 8 JMNHA =JMIN1,JMAX1
     8 F(JMNHA ,N)=1.
       F(JMAX1,N)=1.
       F(JMAX1,NPLUS)=1.
       BURNE (I)=0.
    10 DO 200  JMNHA =JMIN1,JMAX1
       E1=(E(JMNHA ,N)-((P(JMNHA ,N)+Q(JMNHA ,NPLHA ))*
      1(V(JMNHA ,NPLUS )-V(JMNHA ,N))))*.0001/ROZER (I)
       VE=V(JMNHA ,NPLUS )/ROZER (I)
       IF(F(JMNHA ,NPLUS )-1.0) 98,99,99
    98 P1=10.
       GO TO 101
    99 P1=P(JMNHA ,N)*.0001
   101 P1VE=P1*VE
       IF(P1VE-1.0465) 11,11,12
    11 ALPHA=0.0
       DALFD =0.0
       DALFV =0.0
       GO TO 15
    12 IF(P1VE-3.488) 13,13,14
    13 ALPHA=8600.0*P1VE-9000.0
       DALFD =8600.0*VE
       DALFV =8600.0*P1
```

```
      GO TO 15
   14 ALPHA=21.0E03
      DALFD =0.0
      DALFV =0.0
   15 P1VE2=P1VE**2
      P1VE4=P1VE2**2
      P1VE5=P1VE4*P1VE
      BRAC1=1140.0+P1VE4
      BRAC2=.101E-03*ALOG(ABS(P1/1.013E-03))-.2325E-03
      EF=6.57*P1VE+974.0*P1VE2/BRAC1-ALPHA*BRAC2-E1
      EPRIM =6.57*VE+1948.0*VE**2*P1/BRAC1-3896.0*VE*P1VE5/BRAC1**2
     1-DALFD *BRAC2-ALPHA*.101E-03/P1
      PNEW=P1-EF/EPRIM
      IF(ABS(PNEW-P1)-.0001) 17,17,16
   16 P1=PNEW
      GO TO 101
   17 E(JMNHA ,NPLUS )=E1-(.5*(P1*10000.*F(JMNHA ,NPLUS )-P(JMNHA ,N))*
     1(V(JMNHA ,NPLUS )-V(JMNHA ,N)))*.0001/ROZER (I)
  171 P1VE=P1*VE
      P1VE2=P1VE**2
      P1VE4=P1VE2**2
      P1VE5=P1VE4*P1VE
      IF(P1VE-1.0465) 18,18,19
   18 ALPHA=0.0
      DALFD =0.0
      DALFV =0.0
      GO TO 22
   19 IF(P1VE-3.488) 20,20,21
   20 ALPHA=8600.*P1VE-9000.0
      DALFD =8600.0*VE
      DALFV =8600.0*P1
      GO TO 22
   21 ALPHA=21.0E03
      DALFD =0.0
      DALFV =0.0
   22 BRAC1=1140.0+P1VE4
      BRAC2=.101E-03*ALOG(ABS(P1/1.013E-03))-.2325E-03
      EF=6.57*P1VE+974.0*P1VE2/BRAC1-ALPHA*BRAC2-E(JMNHA ,NPLUS )
      EPRIM =6.57*VE+1948.0*VE**2*P1/BRAC1-3896.*VE*P1VE5/BRAC1**2
     1-DALFD *BRAC2-ALPHA*.101E-03/P1
      PNEW=P1-EF/EPRIM
      IF(ABS(PNEW-P1)-.0001) 24,24,23
   23 P1=PNEW
      GO TO 171
   24 E(JMNHA ,NPLUS )=E(JMNHA ,NPLUS )*1.0E04*ROZER (I)
      P(JMNHA ,NPLUS )=P1*1.0E04*F(JMNHA ,NPLUS)
      DEDP=EPRIM
      DEDV=6.57*P1+1948.0*P1VE*P1/BRAC1-3896.0*P1VE5*P1/BRAC1**2
     1-DALFV *BRAC2
      IF(F(JMNHA ,NPLUS ))202,201,202
  201 CSQ(JMNHA )=1.0
      GO TO 200
  202 CSQ(JMNHA )=(V(JMNHA ,NPLUS )/ROZER (I))**2*(P1+DEDV)/DEDP*1.E04
  200 THETA(JMNHA)=P(JMNHA,NPLUS)*V(JMNHA,NPLUS)/(85.    *ROZER(I) *12.
      RETURN
       END
```

```
$IBFTC ETAT2   NOLIST
       SUBROUTINE EQST2
       COMMON AREA1,BRAKE,CSQMA,DLAMA,DTLAS,DUO,EINSU,EKSUM,EMPRO,ESUM,
      1I,IMAX,IQUIT,JLAST,N,N1,N2,NBAR1,NBAR2,NCYCL,NMNHA,NN,NOUTP,
      2NPL3H,NPLHA,NPLUS,PIN3,PINIT,RADIU,SHPR,SIGMA,XBAR1,XSTOP,ZMEXP,
      3T
       COMMON AREA(200,2),BURNE(2),CQSQX(3),CSQ(200),DTMIN(3),DTSQ(200),
      1F(200,2),EINT(3),EKIN(3),F(200,2),HALFM(200),HALFR(3),INTER(4),
      2NZONE(3),P(200,2),PPLUS(200),Q(200,2),ROZER(3),THETA(200),
      3TMINS(2),U(200,2),USQ(200),V(200,2),X(200,2)
       I=1
       JMIN=INTER(I)+1
       JMAX=INTER(I+1)
       JMIN1=JMIN-1
       JMAX1=JMAX-1
       IF(BURNE (I)) 1,10,1
     1 FMIN=2.
       DO 66 JMNHA =JMIN1,JMAX1
       F(JMNHA,NPLUS)=(1.0-V(JMNHA,NPLUS))/(1.0-0.7872)
       IF(F(JMNHA,NPLUS)-.001) 2,3,3
     2 F(JMNHA ,NPLUS )=0.
     3 IF(F(JMNHA ,NPLUS )-1.) 4,6,5
     4 IF(F(JMNHA ,NPLUS )-F(JMNHA ,N)) 5,6,6
     5 F(JMNHA ,NPLUS )=1.
   6   IF(F(JMNHA,NPLUS)-FMIN) 300,300,301
 300   FMIN=F(JMNHA,NPLUS)
       GO TO 66
 301   FMIN=FMIN
  66   CONTINUE
       IF(FMIN-1.) 10,7,7
     7 DO 8 JMNHA =JMIN1,JMAX1
     8 F(JMNHA ,N)=1.
       BURNE (I)=0.
    10 DO 200  JMNHA =JMIN1,JMAX1
       F1=(E(JMNHA ,N)-(P(JMNHA ,N)+Q(JMNHA ,NPLHA ))*(V(JMNHA ,NPLUS )-
      1V(JMNHA ,N)))*1.0E-06/ROZER (I)
       RHO=ROZER (I)/V(JMNHA ,NPLUS )
       RHO2=RHO**2
       EXPON=EXP(-6./RHO)
    20 A= .002164*RHO2*RHO2+2.0755*EXPON
       B=.35*RHO
       DADRH = .008656*RHO*RHO2+12.4530*EXPON/RHO2
       DBDRH =.35
       P1=(A+B*F1 )*1.0E06
   108 E(JMNHA ,NPLUS )=E1*1.0E06*ROZER (I)-.5*(P1-P(JMNHA ,N))*
      1(V(JMNHA ,NPLUS )-V(JMNHA ,N))
       P(JMNHA ,NPLUS )=(A+B*E(JMNHA ,NPLUS )*1.0E-06/ROZER (I))*1.0E06
      1*F(JMNHA ,NPLUS )
       IF(F(JMNHA ,NPLUS ))202,201,202
   201 CSQ(JMNHA )=1.0
       GO TO 200
   202 CSQ(JMNHA )=(B*P(JMNHA ,NPLUS )*1.0E-06/RHO2+DADRH +DBDRH*
      1E(JMNHA ,NPLUS )*1.0E-06/ROZER (I))*1.0E06
   200 THETA(JMNHA)=P(JMNHA,NPLUS)*V(JMNHA,NPLUS)/(3.144*ROZER(I))
       RETURN
       END
```

```
$IBFTC ETAT3   NOLIST
       SUBROUTINE EQST3
       REAL MU,MU0,MU2
       COMMON AREA1,BRAKE,CSQMA,DLAMA,DTLAS,DUO,EINSU,EKSUM,EMPRO,ESUM,
      1II,IMAX,IQUIT,JLAST,N,N1,N2,NBAR1,NBAR2,NCYCL,NMNHA,NN,NOUTP,
      2NPL3H,NPLHA,NPLUS,PIN3,PINIT,RADIU,SHPR,SIGMA,XBAR1,XSTOP,ZMEXP,
      3T
       COMMON AREA(200,2),BURNE(2),CQSQX(3),CSQ(200),DTMIN(3),DTSQ(200),
      1E(200,2),EINT(3),EKIN(3),F(200,2),HALFM(200),HALFR(3),INTER(4),
      2NZONE(3),P(200,2),PPLUS(200),Q(200,2),ROZER(3),THETA(200),
      3TMINS(2),U(200,2),USQ(200),V(200,2),X(200,2)
       I=3
       JMIN=INTER(I)+1
       JMAX=INTER(I+1)
       JMIN1=JMIN-1
       JMAX1=JMAX-1
       DO 200 JMNHA=JMIN1,JMAX1
       E1=(E(JMNHA,N)-((P(JMNHA,N)+Q(JMNHA,NPLHA))*(V(JMNHA,NPLUS)
      1-V(JMNHA,N))))/(1960.0*ROZER(I))
       P1=P(JMNHA,N)/1.01375
       HETA=ROZER(3)/(V(JMNHA,NPLUS)*1.293E-03)
       PSI=ALOG(HETA)
       Z1=P1/HETA
       NE=1
  1    Y=1.0/Z1
       A=(25.8948684*Y+3.0)/(4.77897369*Y+1.0)
       DADY=11.5579473/(4.77897369*Y+1.0)**2
       B=861.0*Y*(1.0-Y)/(3000.0*Y**2+1.0)
       DBDY=861.0*(1.0-2.0*Y)/(3000.0*Y**2+1.0)
      1-0.5166E+07*Y**2*(1.0-Y)/(3000.0*Y**2+1.0)**2
       C=2536.0*Y*(1.0-Y)/(0.9E+05*Y**2+1.0)
       DCDY=2536.0*(1.0-2.0*Y)/(0.9E+05*Y**2+1.0)
      1-0.45648E+09*Y**2*(1.0-Y)/(0.9E+05*Y**2+1.0)**2
       D=0.41E+05*(1.0-Y)*Y/(0.12E+08*Y**2+1.0)
       DDDY=0.41E+05*(1.0-2.0*Y)/(0.12E+08*Y**2+1.0)
      1-0.984E+10*Y**2*(1.0-Y)/(0.12E+08*Y**2+1.0)**2
       MU0=1.0+A+B+C+D
       DMU0Y=DADY+DBDY+DCDY+DDDY
       MU2=(6002.0*Y+4.0)/(1000.0*Y+1.0)
       DMU2Y=2002.0/(1000.0*Y+1.0)**2
       MU=MU0+0.09*(MU0-MU2)*PSI
       DMUY=(1.0+0.09*PSI)*DMU0Y-0.09*PSI*DMU2Y
       DMU=-DMUY*Y**2
       EF=0.20*Z1*(MU-1.0)-E1
       EPRIM=0.20*(MU-1.0+Z1*DMU)
       ZNEW=Z1-EF/EPRIM
       IF(ABS(ZNEW-Z1)-.00001) 3,3,2
  2    Z1=ZNEW
       GO TO 1
  3    IF(NE-1) 4,4,5
  4    P1=1.01375*HETA*Z1
       E1=E1-(0.5*((P1-P(JMNHA,N))*(V(JMNHA,NPLUS)-V(JMNHA,N))))/(1960.0
      1*ROZER(I))
       NE=2
       GO TO 1
  5    E(JMNHA,NPLUS)=1960.0*ROZER(I)*E1
       P(JMNHA,NPLUS)=1.01375*HETA*Z1
       S=485.0/(1000.0+Z1**2)+3860.0    /(7500.0+16.5*Z1)
       THETA(JMNHA)=273.2*Z1*S
  200  CSQ(JMNHA)=1.40*P(JMNHA,NPLUS)*V(JMNHA,NPLUS)/ROZER(I)
       RETURN
       END
```

SUBROUTINE LIRE

This subroutine reads the necessary data to start the program. There are 12 input data cards.

- 1st card — IMAX: has to be taken as 3 in the present version of the program; no other choice is possible
- 2nd card — AREA1: area of the barrel in cm^2.
  RADIU: radius of the barrel in cm.
  XSTOP: length at which the program is to be stopped.
- 3rd card — EMPRO: mass of the projectile in g.
- 4th card — ZMEXP: mass of explosive in g.
- 5th card — PINIT: initial pressure of the gas mixture in PSIA
- 6th card — SHPR : pressure at which the diaphragm bursts in bars.
- 7th card — PIN3 : initial pressure in the barrel in Torr.
- 8th card — NZONE(1): number of zones in region I (I = 1 and 2).
- 9th card — XBAR1: length of the barrel divided in NBARI zones.
- 10th card — NBARI: number of zones in the first part of the barrel.
  NBAR2: number of zones in the remaining part of the barrel.
- 11th card — N1: cycle number of the first output.
  N2: cycle interval between two outputs.
- 12th card — DUO: if DUO $\leq$ 0, program is to exit after completion, if DUO > 0 another run is to be done

Set of sample data.

MAIN PROGRAM

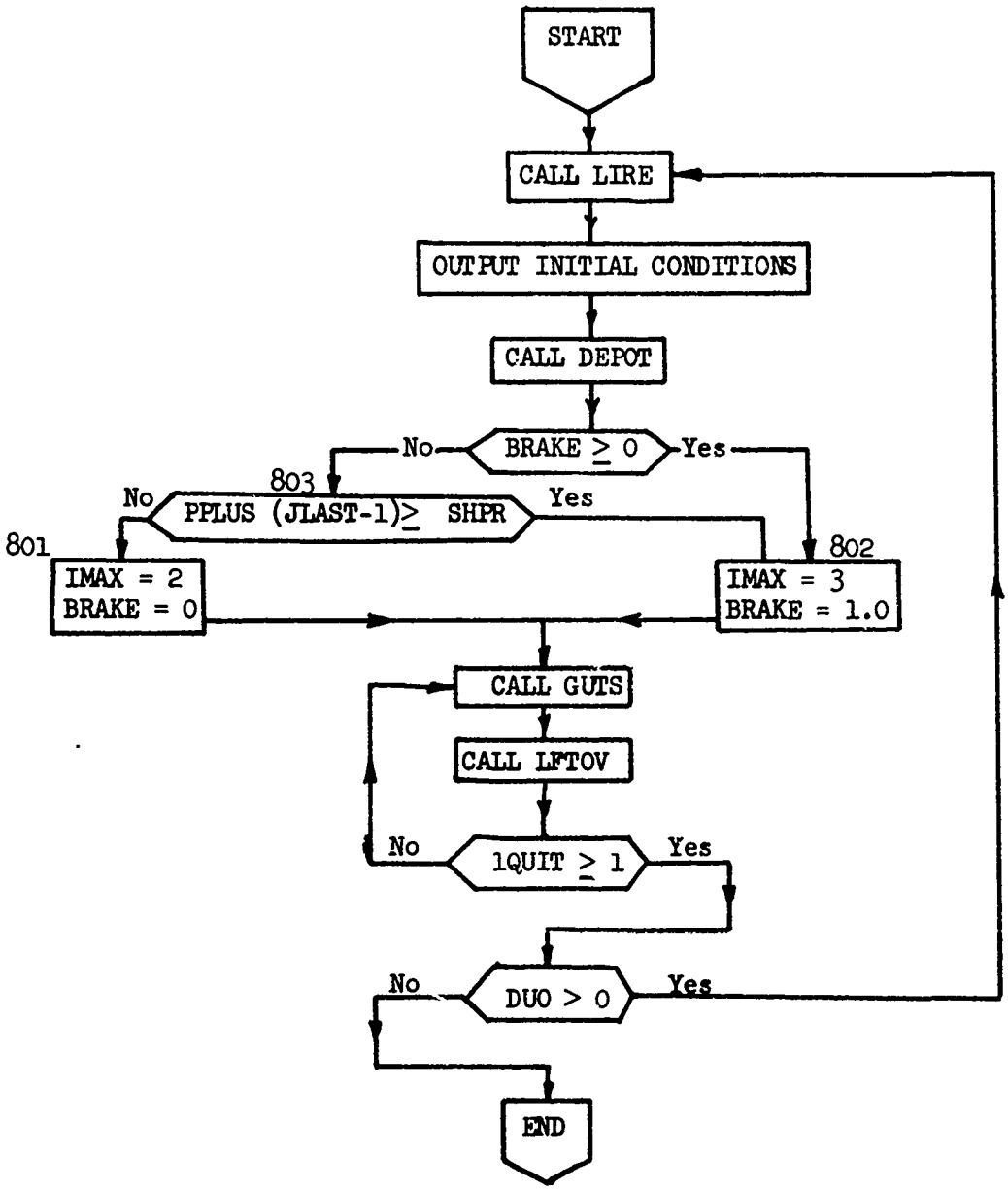

SUBROUTINE DEPOT

The initial conditions for the problem are set up in this subroutine

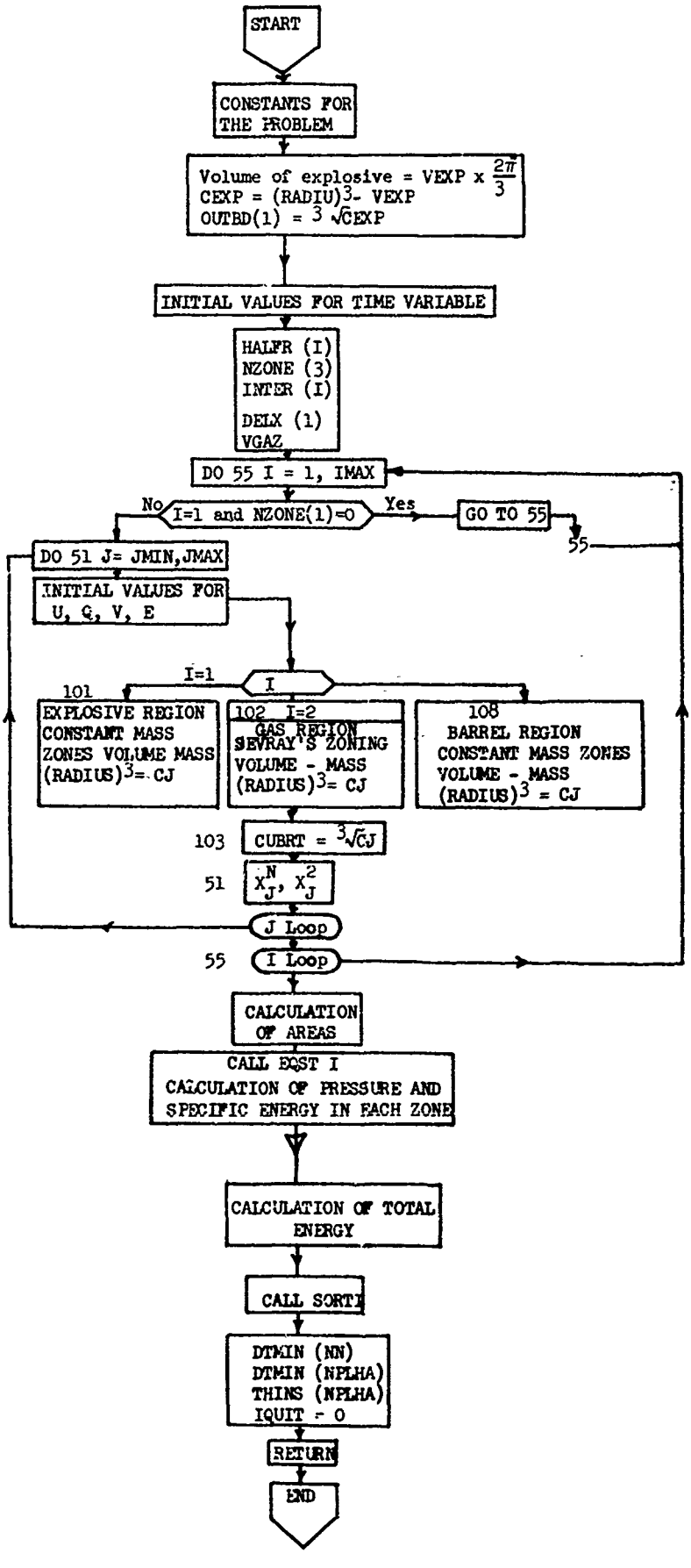

SUBROUTINE GUTS

This subroutine calculates new variables for each time step

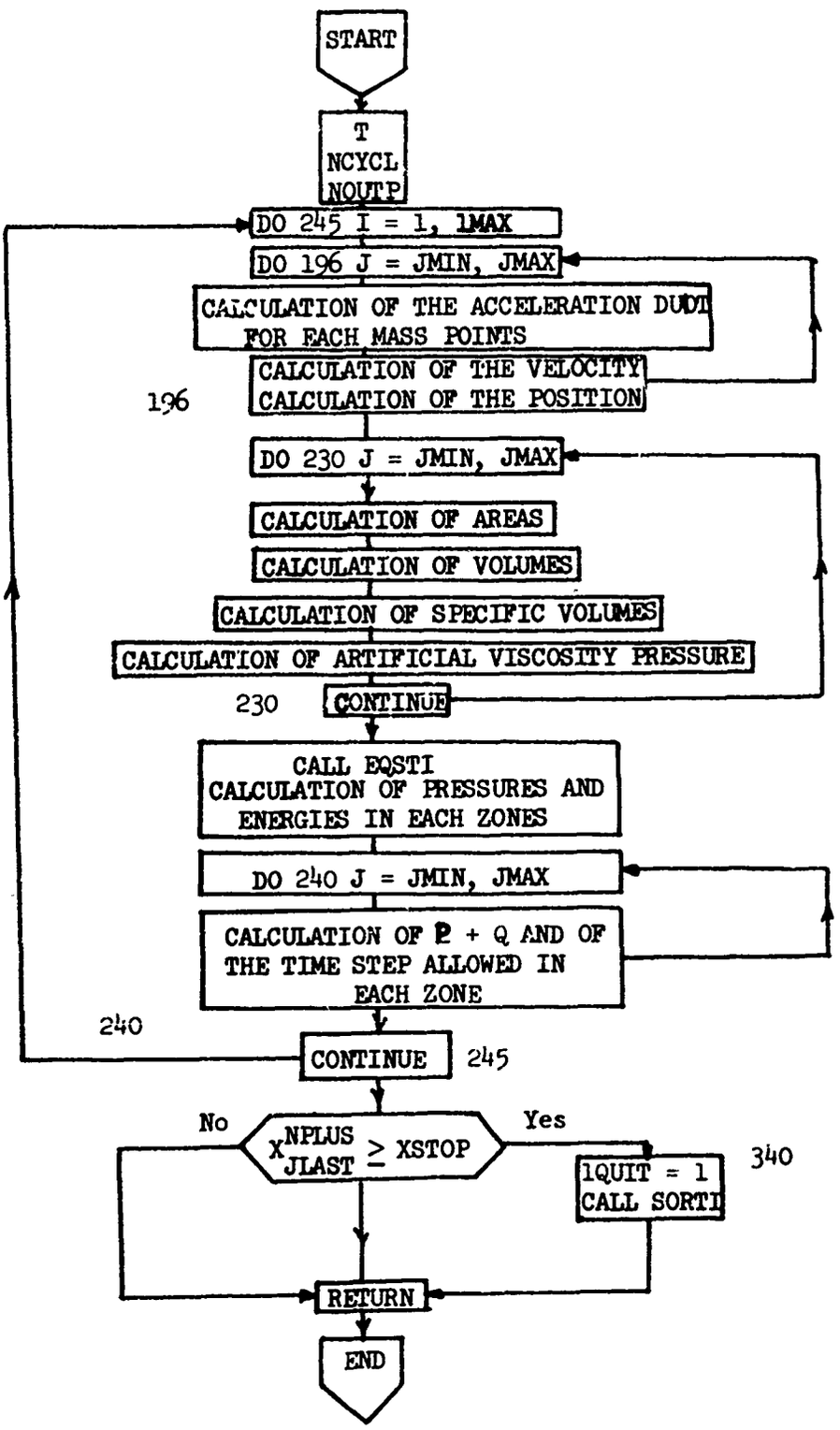

SUBROUTINE LFTOV

New time steps are determined and total energy is calculated

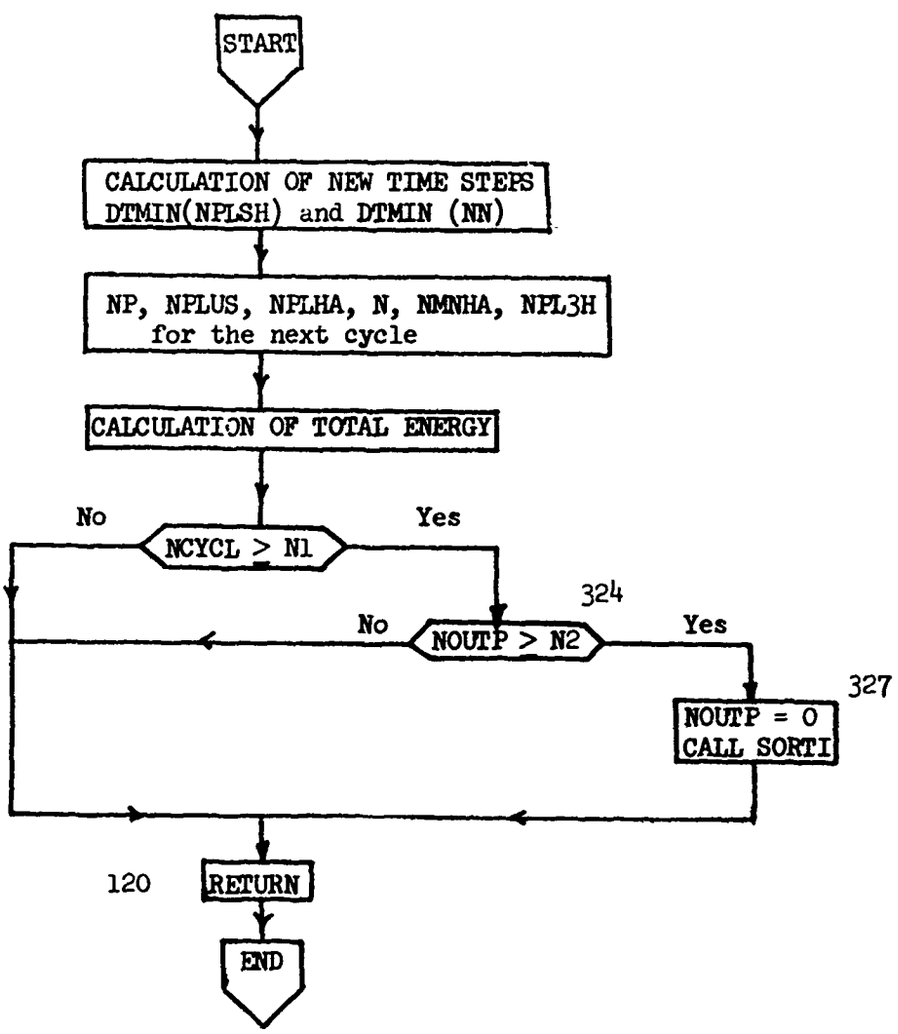

SUBROUTINE SORTI

This subroutine provides printed output when print-out cycle is reached.

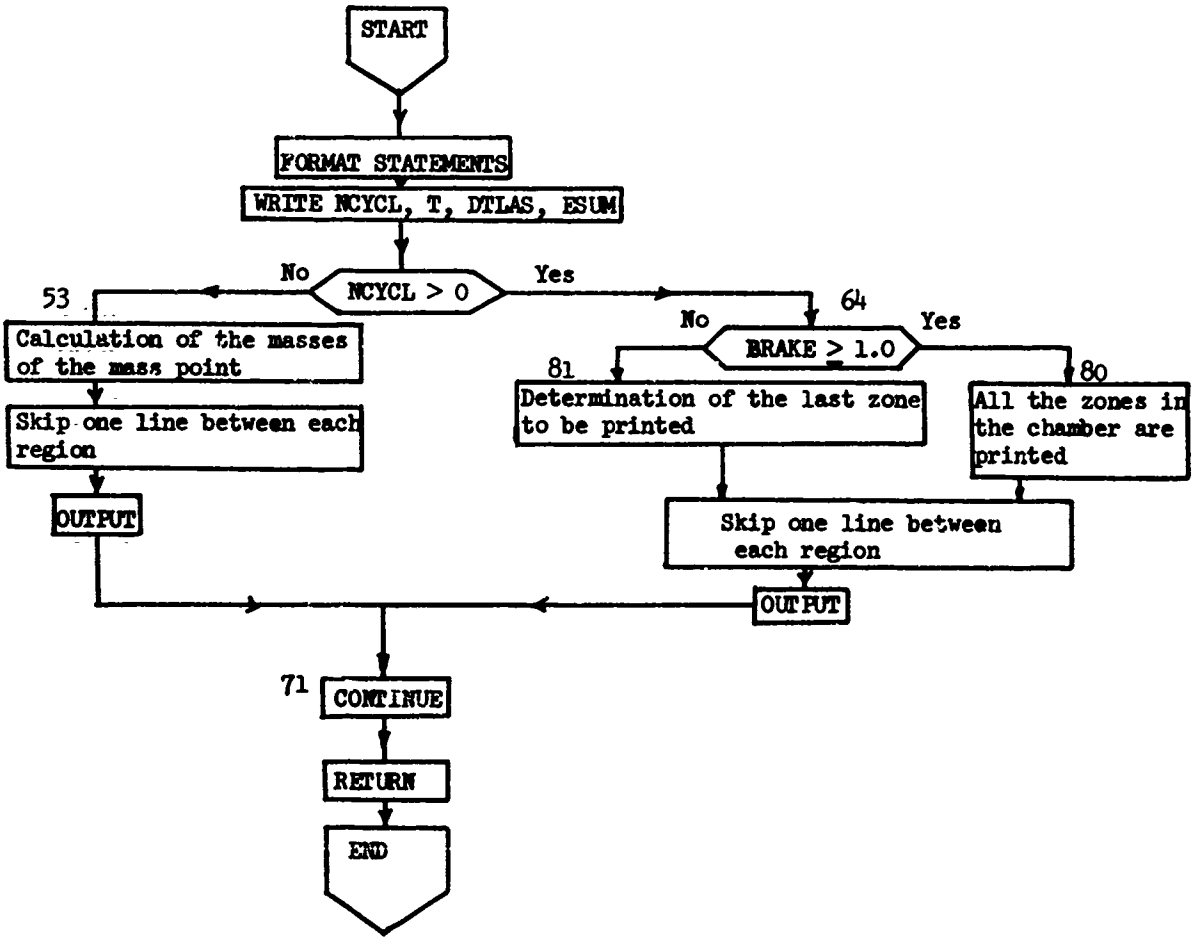

SUBROUTINE EQST1

Equation of state for gas mixture $2H_2 + O_2$ (see Sec. 2.3.1)

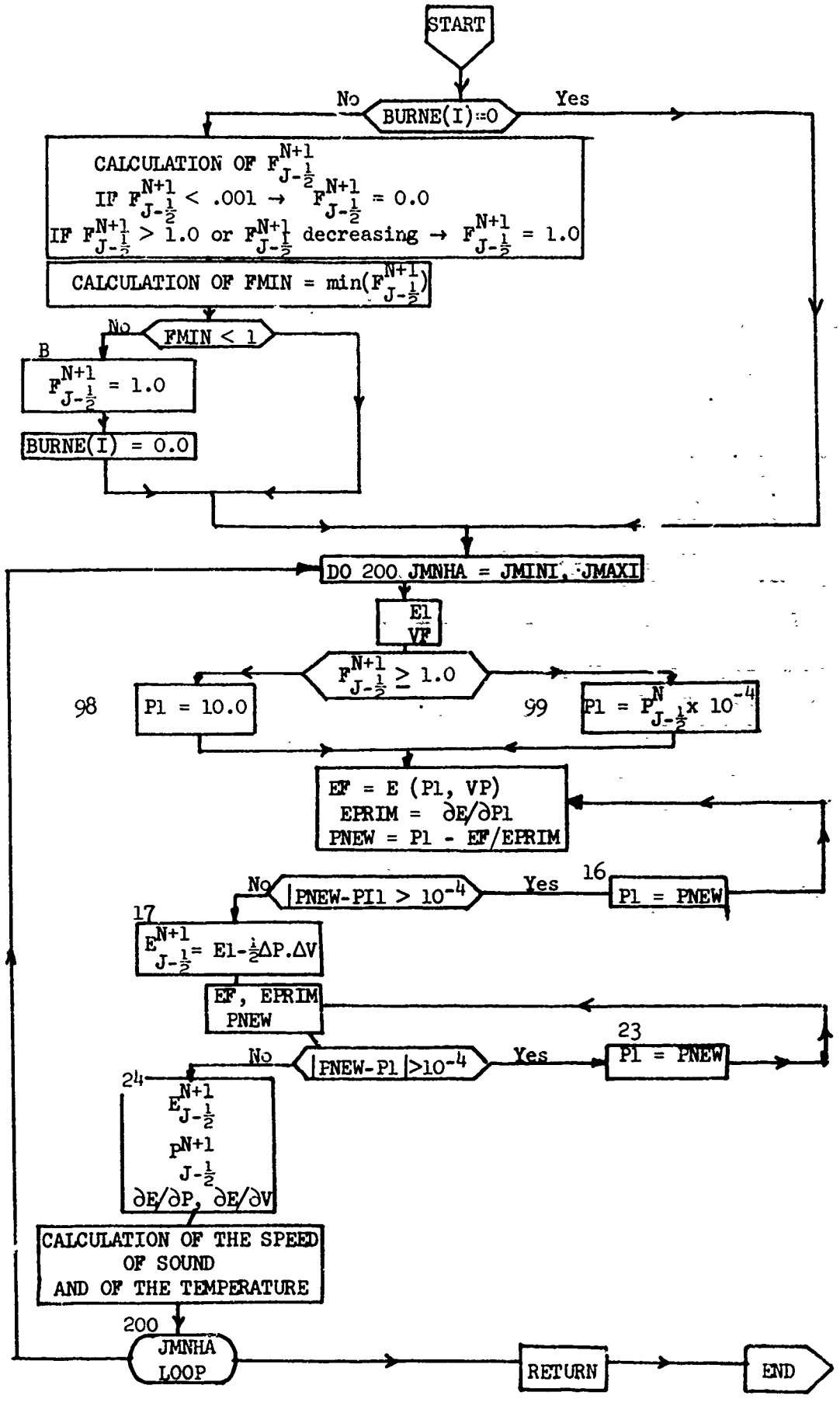

SUBROUTINE EQST2

Equation of state for explosive (see Sec.2.3.2)

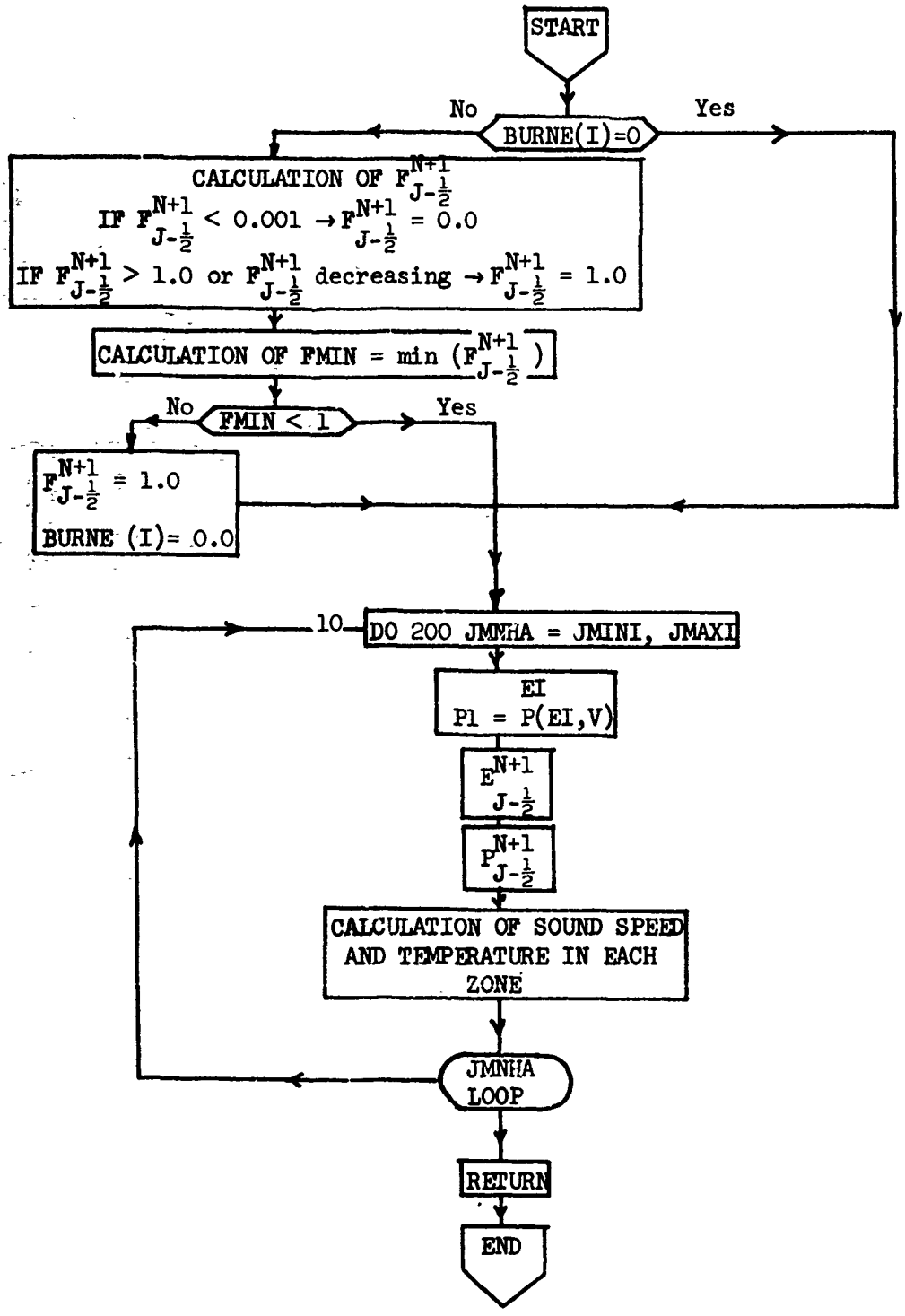

SUBROUTINE EQST3

Equation of state for air (see Sec. 2.3.3)